

COORDINATES FOR  $SL_3$ -WEB BASIS ELEMENTS IN CLOSED SURFACES

ZHE SUN AND ZHIHAO WANG

ABSTRACT. The  $SL_3$ -skein algebra of a closed surface  $\Sigma_g$  is a quantization of the  $SL_3$  character variety of  $\Sigma_g$ , where  $g$  denotes the genus of the surface. This algebra admits a basis consisting of non-elliptic web diagrams in  $\Sigma_g$ . In this paper, we introduce explicit coordinates for non-elliptic web diagrams on  $\Sigma_g$ , yielding a parametrization by a submonoid of  $\mathbb{Z}^d$ . Here  $d = 16g - 16$  for  $g \geq 2$  and  $d = 4$  in the torus case  $g = 1$ , coinciding with the dimension of the corresponding character variety.

## CONTENTS

1. Introduction	1
1.1. Background	1
1.2. Main results	2
2. The $SL_3$ -skein algebra	4
2.1. $SL_3$ -skein algebras	5
2.2. Bases of the $SL_3$ -skein algebras	6
2.3. Graded $SL_3$ -skein algebras	6
3. Unbounded $SL_3$ -laminations and their shear coordinates	7
3.1. Unbounded $SL_3$ -laminations	7
3.2. $SL_3$ -shear coordinates	10
4. General positions of basis elements in pants decompositions of a closed surface	11
5. Webs in an annulus	13
5.1. Braids and braided webs in the annulus	14
5.2. Non-elliptic web diagrams in the annulus	15
5.3. Twist numbers	20
6. Webs in a pair of pants	21
7. Coordinates for non-elliptic $SL_3$ web diagrams on closed surfaces	24
7.1. The genus is more than one	24
7.2. The closed torus	28
References	29

## 1. INTRODUCTION

We will use  $\mathbb{Z}$  and  $\mathbb{N}$  to denote the set of integers and the set of non-negative integers respectively. Let  $R$  be a commutative domain with an invertible element  $q^{\frac{1}{3}}$ .

**1.1. Background.** The  $(SL_3)$  webs were introduced by Kuperberg to study the representation theory of  $\mathfrak{sl}_3$  [Kup96]. An  $SL_3$  web is a finite oriented trivalent graph whose each vertex is either a sink or a source (see Definition 2.2).

---

*Key words and phrases.*  $SL_3$ -skein algebras, closed surfaces, bases coordinates.

Let  $\Sigma$  be a punctured surface, that is, a surface obtained from a closed surface by removing finitely many points. The  $\mathrm{SL}_3$ -skein algebra  $\mathcal{S}(\Sigma)$  [MOY98, Sik01, SW07] is defined as the quotient  $R$ -module of the free  $R$ -module generated by isotopy classes of  $\mathrm{SL}_3$  webs embedded in  $\Sigma \times (-1, 1)$ , modulo the local relations (3)-(8). The algebra structure on  $\mathcal{S}(\Sigma)$  is given by stacking: for two  $\mathrm{SL}_3$  webs  $W_1$  and  $W_2$  in  $\Sigma \times (-1, 1)$ , their product  $W_1 W_2$  is defined by placing  $W_1$  above  $W_2$ .

It was shown in [SW07] that the  $\mathrm{SL}_3$ -skein algebra  $\mathcal{S}(\Sigma)$  admits a basis  $B_\Sigma$  consisting of all non-elliptic web diagrams in  $\Sigma$ , where two web diagrams are identified if they represent isotopic  $\mathrm{SL}_3$  webs in  $\Sigma \times (-1, 1)$ . A non-elliptic web diagram is a crossingless web diagram that contains none of the following faces:



When each connected component of  $\Sigma$  contains at least one puncture and  $\Sigma$  admits a triangulation, the basis elements in  $B_\Sigma$  are parametrized by a submonoid of  $\mathbb{Z}^d$  [FS22, DS24], where  $d$  is the dimension of the corresponding character variety. Moreover, the coordinates defined in [DS24] with respect to different triangulations are shown in [DS25] that they are related by a sequence of tropical cluster transformations [FG06].

The parametrization of basis elements in  $B_\Sigma$  plays a central role in the study of the  $\mathrm{SL}_3$ -skein algebra. Such parametrizations have important applications, including the study of the center and representation theory of  $\mathrm{SL}_3$ -skein algebras [KW24], the construction of quantum trace maps and identification of the highest term exponents of the quantum trace with the coordinates [Kim20], among others.

The  $\mathrm{SL}_3$ -skein algebra is a special case of the  $\mathrm{SL}_n$ -skein algebra introduced in [MOY98, Sik01]. When  $n = 2$ , this construction recovers the well-known Kauffman bracket skein algebra [Tur88, Tur89]. In this case, the set of crossingless multi-curves on a closed surface forms a basis of the  $\mathrm{SL}_2$ -skein algebra [PS00], and these basis elements are parametrized by the classical Dehn–Thurston coordinates (see e.g. [LS04]). The motivation of this paper is to extend the theory of Dehn–Thurston coordinates from the  $\mathrm{SL}_2$  setting to the  $\mathrm{SL}_3$ -skein algebra. Since the Dehn–Thurston coordinates could be considered as the tropicalization of the Fenchel–Nielsen coordinates of the Teichmüller space, our new coordinates should be considered as the tropicalization of the generalized Fenchel–Nielsen coordinates [CJK21, Kim99, SWZ20] for the moduli space of convex  $\mathbb{RP}^2$  structures [FG07, Gol90].

Let us now describe our new coordinates in more details. For each positive integer  $g$ , let  $\Sigma_g$  denote the closed surface of genus  $g$ . To construct coordinates for non-elliptic web diagrams in  $\Sigma_g$ , we distinguish two cases:  $g \geq 2$  and  $g = 1$ .

**1.2. Main results.** When  $g \geq 2$ , as in the  $\mathrm{SL}_2$  setting, the construction of coordinates for non-elliptic web diagrams in  $\Sigma_g$  requires a pants decomposition of  $\Sigma_g$ . A *pants decomposition* of  $\Sigma_g$  is a collection of nontrivial simple closed curves  $\{C_j\}_{j=1}^r$  on  $\Sigma_g$ , where  $r = 3g - 3$ . We call the decomposition *oriented* if each curve  $C_j$  is endowed with an orientation.

For each  $j = 1, \dots, r$ , let  $N(C_j)$  be a small closed annular neighborhood of  $C_j$  in  $\Sigma_g$ . Removing  $\bigsqcup_{j=1}^r \mathrm{Int} N(C_j)$  from  $\Sigma_g$  yields a surface that is a disjoint union of pairs of pants. We use  $\mathbb{P}$  to denote the set of these pairs of pants.

A *dual graph* is a trivalent graph  $\Gamma$  embedded in  $\Sigma_g$  such that each curve  $C_j$  ( $j = 1, \dots, r$ ) intersects  $\Gamma$  in exactly one point, and the intersection of  $\Gamma$  with each pair of pants consists of a single trivalent vertex.

For each  $1 \leq j \leq r$ , let  $\mathcal{N}_j$  denote the surface

$$\mathcal{N}_j = N(C_j) \setminus (\partial N(C_j) \cap \Gamma).$$

To define global coordinates for a non-elliptic web diagram  $W$  in  $\Sigma_g$ , we first place  $W$  in general position with respect to the oriented pants decomposition  $\{C_j\}_{j=1}^r$  (Definition 4.2). We then define local coordinates for each intersection  $W \cap \mathcal{N}_j$ ,  $1 \leq j \leq r$ , and for each intersection  $W \cap P$ , where  $P \in \mathbb{P}$ .

We depict  $\mathcal{N}_j$  as in Figure 20, where the red oriented curve represents  $C_j$ . An *increasing* (resp. *decreasing*) curve is an oriented curve in  $\mathcal{N}_j$  connecting the two boundary components of  $\mathcal{N}_j$  whose orientation is always from left to right (resp. from right to left).

To define the local coordinates for  $W \cap \mathcal{N}_j$ , we classify the web diagrams  $W \cap \mathcal{N}_j$  into two types (Lemma 5.4 and Proposition 5.5): strict minimal braided webs (Definition 5.1) and line-circle webs (Figure 11). As noted in Definition 5.1, a minimal braided web in  $\mathcal{N}_j$  is obtained from a unique minimal strict braid in  $\mathcal{N}_j$ , which consists of a collection of increasing and decreasing curves in  $\mathcal{N}_j$ .

When  $W \cap \mathcal{N}_j$  is a strict minimal braided web obtained from a minimal strict braid in  $\mathcal{N}_j$ , suppose this minimal strict braid consists of increasing curves  $\{c_1, \dots, c_m\}$  and decreasing curves  $\{d_1, \dots, d_l\}$ . We define

$$\begin{aligned} t_{j1}(W) &:= \text{the sum of the twist numbers of the curves } \{c_1, \dots, c_m\}, \\ t_{j2}(W) &:= \text{the sum of the twist numbers of the curves } \{d_1, \dots, d_l\}, \end{aligned} \quad (1)$$

where the twist number of a curve is defined as in Figure 10.

When  $W \cap \mathcal{N}_j$  is a line-circle web, we define

$$(t_{j1}(W), t_{j2}(W)) = \begin{cases} (t, m), & \text{if } W \cap \mathcal{N}_j \text{ is the left configuration in Figure 11,} \\ (m, t), & \text{if } W \cap \mathcal{N}_j \text{ is the right configuration in Figure 11.} \end{cases} \quad (2)$$

Theorem 5.10 shows that the pair  $(t_{j1}(W), t_{j2}(W))$ , together with the two intersection numbers (Definition 5.8) and the signature of  $W \cap \mathcal{N}_j$  (see (30)), uniquely determines  $W \cap \mathcal{N}_j$ .

We may regard each pair of pants  $P \in \mathbb{P}$  as a third-punctured sphere  $\Sigma_{0,3}$ , as illustrated in Figure 4. Then  $W \cap P$  can be viewed as an unbounded lamination in  $\Sigma_{0,3}$  (see §3.1). Let  $I(\Sigma_{0,3})$  denote the set of eight vertices in  $\Sigma_{0,3}$  labeled by 11, 12, 21, 22, 31, 32,  $v$ ,  $v'$  as in Figure 4.

In [IK25], the authors defined the shear coordinates of  $W \cap P$  (Lemma 3.9)

$$\mathbf{x}(W \cap P) = (x_{11}, x_{12}, x_{21}, x_{22}, x_{31}, x_{32}, x_v, x_{v'}) \in \mathbb{Z}^{I(\Sigma_{0,3})}.$$

We then define

$$\begin{aligned} t_P(W) &= x_v - x_{v'}, \\ h_P(W) &= x_{11} - x_{12} + x_{21} - x_{22} + x_{31} - x_{32}. \end{aligned}$$

Proposition 6.2 and Theorem 6.3 together imply that the pair  $(t_P(W), h_P(W))$ , together with the six intersection numbers (Definition 6.1), uniquely determines  $W \cap P$  up to the moves shown in Figure 22.

Let  $C$  be an oriented closed curve in  $\Sigma$ . We say that a web diagram  $W$  is in *minimal intersection position* with respect to  $C$  if the intersection number between  $W$  and  $C$  is minimal.

Assume that  $W$  is in minimal intersection position with respect to  $C$ . By placing  $C$  above  $W$ , we define

$$\begin{aligned} i_1(C, W) &:= \text{the number of positive crossings between } C \text{ and } W, \\ i_2(C, W) &:= \text{the number of negative crossings between } C \text{ and } W. \end{aligned}$$

Proposition 5.5 shows that  $i_1(C, W)$  and  $i_2(C, W)$  are well defined.

For each  $1 \leq j \leq r$ , we then define

$$n_{j1}(W) := i_1(C_j, W), \quad n_{j2}(W) := i_2(C_j, W).$$

We now state our first main theorem, which parametrizes the non-elliptic web diagrams in  $B_{\Sigma_g}$  for  $g \geq 2$  by a submonoid of  $\mathbb{Z}^{16g-16}$ , where  $16g-16$  is the dimension of the corresponding character variety.

**Theorem 1.1.** *Let  $\{C_j\}_{1 \leq j \leq r}$  be an oriented pants decomposition of  $\Sigma_g$  with  $g \geq 2$ , together with a dual graph  $\Gamma$ , where  $r = 3g - 3$ . The coordinate map*

$$\kappa: B_{\Sigma_g} \longrightarrow \mathbb{N}^r \times \mathbb{N}^r \times \mathbb{Z}^r \times \mathbb{Z}^r \times \mathbb{Z}^{\mathbb{P}} \times \mathbb{Z}^{\mathbb{P}},$$

$$W \mapsto \left( (n_{j1}(W))_{1 \leq j \leq r}, (n_{j2}(W))_{1 \leq j \leq r}, (t_{j1}(W))_{1 \leq j \leq r}, (t_{j2}(W))_{1 \leq j \leq r}, (t_P(W))_{P \in \mathbb{P}}, (h_P(W))_{P \in \mathbb{P}} \right)$$

is injective. Moreover,

$$\text{Im } \kappa = \Theta,$$

where  $\Theta$  is the submonoid of  $\mathbb{N}^r \times \mathbb{N}^r \times \mathbb{Z}^r \times \mathbb{Z}^r \times \mathbb{Z}^{\mathbb{P}} \times \mathbb{Z}^{\mathbb{P}}$  defined in Definition 7.3.

When  $g = 1$ , that is, when the closed surface  $\Sigma_g$  is the torus  $\Sigma_1$ , there is no pants decomposition. Instead, we define coordinates for non-elliptic web diagrams in  $\Sigma_1$  using an oriented closed curve  $\gamma \subset \Sigma_1$  together with a fixed point  $p \in \gamma$ .

A non-elliptic web diagram  $W$  in  $\Sigma_1$  is said to be in *general position* with respect to  $\gamma$  if  $W$  is in minimal intersection position with  $\gamma$  and satisfies  $p \notin W$ .

Cutting  $\Sigma_1$  along  $\gamma$  and taking the closure yields an annulus, which we denote by  $\mathbb{A}_\gamma$ . The point  $p$  gives rise to two points  $p', p'' \in \partial \mathbb{A}_\gamma$ , one on each boundary component. We set

$$\mathbb{A}'_\gamma := \mathbb{A}_\gamma \setminus \{p', p''\}.$$

Let  $W_\gamma$  denote the web diagram in  $\mathbb{A}'_\gamma$  obtained from  $W$  by cutting along  $\gamma$ .

The orientation of  $\gamma$  induces orientations on the two boundary components of  $\mathbb{A}'_\gamma$ . There is a unique identification of  $\mathbb{A}'_\gamma$  with the annulus in Figure 20 such that the induced orientations of the boundary components of  $\mathbb{A}'_\gamma$  agree with the orientation of the red curve in Figure 20. Using this identification, we define the twist coordinates  $(t_1(W), t_2(W))$  from  $W_\gamma$  as in (1) and (2).

We further define the intersection coordinates

$$n_1(W) := i_1(\gamma, W), \quad n_2(W) := i_2(\gamma, W).$$

We now state our second main theorem, which parametrizes the non-elliptic web diagrams on  $\Sigma_1$  by a submonoid of  $\mathbb{Z}^4$ .

**Theorem 1.2.** *Let  $\gamma$  be an oriented closed curve in  $\Sigma_1$ , and fix a point  $p \in \gamma$ . The coordinate map*

$$\kappa: B_{\Sigma_1} \longrightarrow \mathbb{N}^2 \times \mathbb{Z}^2, \quad W \longmapsto (n_1(W), n_2(W), t_1(W), t_2(W))$$

is injective. Moreover,

$$\text{Im } \kappa = \left\{ (n_1, n_2, t_1, t_2) \in \mathbb{N}^2 \times \mathbb{Z}^2 \mid t_i \geq 0 \text{ whenever } n_i = 0, i = 1, 2 \right\}.$$

The coordinates developed in Theorems 1.1 and 1.2 have potential applications to the study of the domain property, the Frobenius map [KLW25, Hig25], and the center of the  $\text{SL}_3$ -skein algebra of closed surfaces, as well as to  $\text{SL}_3$ -Teichmüller theory [FG06]. We plan to investigate these directions in future work.

**Acknowledgements:** Z. W. is supported by a KIAS Individual Grant (MG104701) at the Korea Institute for Advanced Study. Z. S. is supported by the NSFC grant 12471068. We thank Tsukasa Ishibashi and Thang T. Q. Lê for helpful discussions.

## 2. THE $\text{SL}_3$ -SKEIN ALGEBRA

In this section, we review  $\text{SL}_3$ -skein algebras in [FS22].

**2.1.  $SL_3$ -skein algebras.** A *uni-trivalent graph*  $\alpha$  is a finite graph whose vertices all have valency either one or three. We also allow loop components, that is, connected components without vertices. An *orientation* of a uni-trivalent graph is an assignment of an orientation to each edge and each loop such that every trivalent vertex is either a *source* or a *sink*. The *boundary* of  $\alpha$ , denoted by  $\partial\alpha$ , is the set of 1-valent vertices of  $\alpha$ . Each point of  $\partial\alpha$  is called an *endpoint* of  $\alpha$ .

**Definition 2.1.** A **marked surface**  $\Sigma$  is a surface obtained from an oriented compact surface  $\bar{\Sigma}$ , possibly with boundary circles, by removing a finite set  $\mathcal{M}$  of points. The elements of  $\mathcal{M}$  are called **marked points** of  $\Sigma$ , and those lying in the interior of  $\bar{\Sigma}$  are called the **punctures** of  $\Sigma$ , denoted by  $\dot{\mathcal{M}}$ .

If  $\Sigma$  has empty boundary, we say that  $\Sigma$  is a **punctured surface**. A punctured surface is called a **closed surface** if it contains no punctures.

Let  $\Sigma$  be a marked surface and define

$$\tilde{\Sigma} := \Sigma \times (-1, 1).$$

We call  $\tilde{\Sigma}$  the *thickening* of  $\Sigma$ , or a *thickened surface*. For a point  $x \in \Sigma \times (-1, 1)$ , we refer to its second coordinate (that is, its component in  $(-1, 1)$ ) as the *height* of  $x$ .

**Definition 2.2.** Let  $\Sigma$  be a marked surface. A **web** in  $\tilde{\Sigma}$  is a properly embedded oriented uni-trivalent graph  $\alpha$ . We require the following conditions for  $\alpha$ :

- (W1)  $\alpha$  is equipped with a transversal framing.
- (W2) The set of half-edges at each 3-valent vertex is equipped with a cyclic order.
- (W3) For each connected component  $b$  of  $\partial\Sigma$ , the endpoints of  $\alpha$  lying over  $b \times (-1, 1)$ , if there are any, have mutually distinct heights;
- (W4) The framing of  $\alpha$  at each endpoint of  $\alpha$  is parallel to the  $(-1, 1)$  factor and points toward the positive direction of  $(-1, 1)$ .

We will consider webs in  $\tilde{\Sigma}$  up to isotopy. The emptyset  $\emptyset$  is also considered as a web in  $\tilde{\Sigma}$ . We have the convention that  $\tilde{\Sigma}$  is isotopic only to itself.

Any web  $\alpha$  in  $\tilde{\Sigma}$  can be represented by a **web diagram** in  $\Sigma$ . The diagram is just the projection of  $\alpha$  on  $\Sigma$ . Before projecting, we isotope  $\alpha$  such that the framing is given by the positive direction of  $(-1, 1)$  and at each singular point there are two transversal strands with over-crossing or under-crossing information. At every 3-valent vertex, the cyclic order of half-edges as the image of the web diagram is given by the positive orientation of  $\Sigma$  (drawn counter-clockwise in pictures).

Our ground ring is a commutative domain  $R$  with an invertible element  $q^{\frac{1}{3}}$ .

The  $SL_3$ -skein module of  $\Sigma$ , denoted as  $\mathcal{S}(\Sigma)$ , is the quotient module of the  $R$ -module freely generated by the set of all isotopy classes of webs in  $\tilde{\Sigma}$  subject to relations (3)-(9).

$$\begin{array}{c} \text{Diagram 1} \\ \text{Diagram 2} \end{array} = q^{-\frac{1}{3}} \begin{array}{c} \text{Diagram 3} \\ \text{Diagram 4} \end{array} + q^{\frac{2}{3}} \begin{array}{c} \text{Diagram 5} \\ \text{Diagram 6} \end{array}, \quad (3)$$

$$\begin{array}{c} \text{Diagram 1} \\ \text{Diagram 2} \end{array} = q^{\frac{1}{3}} \begin{array}{c} \text{Diagram 3} \\ \text{Diagram 4} \end{array} + q^{-\frac{2}{3}} \begin{array}{c} \text{Diagram 5} \\ \text{Diagram 6} \end{array}, \quad (4)$$

$$\begin{array}{c} \text{Diagram 1} \\ \text{Diagram 2} \end{array} = \begin{array}{c} \text{Diagram 3} \\ \text{Diagram 4} \end{array} + \begin{array}{c} \text{Diagram 5} \\ \text{Diagram 6} \end{array}, \quad (5)$$

$$\begin{array}{c} \text{Diagram 1} \\ \text{Diagram 2} \end{array} = \begin{array}{c} \text{Diagram 3} \\ \text{Diagram 4} \end{array} + \begin{array}{c} \text{Diagram 5} \\ \text{Diagram 6} \end{array}, \quad (6)$$



FIGURE 1. A flip move.

$$\begin{array}{|c|} \hline \text{---} \circlearrowleft \text{---} \\ \hline \end{array} = -(q + q^{-1}) \begin{array}{|c|} \hline \text{---} \text{---} \\ \hline \end{array}, \quad (7)$$

$$\begin{array}{|c|} \hline \text{---} \circlearrowright \text{---} \\ \hline \end{array} = \begin{array}{|c|} \hline \text{---} \circlearrowleft \text{---} \\ \hline \end{array} = (q^2 + 1 + q^2) \begin{array}{|c|} \hline \text{---} \text{---} \\ \hline \end{array}, \quad (8)$$

$$\begin{array}{|c|} \hline \text{---} \text{---} \\ \hline \end{array} = \begin{array}{|c|} \hline \text{---} \text{---} \\ \hline \end{array} = 0, \quad (9)$$

where each shaded rectangle in the above relations represents an embedded disk in  $\Sigma$ . In each relation, the web diagrams coincide outside this disk.

Then  $\mathcal{S}(\Sigma)$  admits an algebra structure. For any two webs  $\alpha_1$  and  $\alpha_2$  in  $\tilde{\Sigma}$ , we define  $\alpha_1\alpha_2 \in \mathcal{S}(\Sigma)$  to be the result of stacking  $\alpha_1$  above  $\alpha_2$ . We then refer to  $\mathcal{S}(\Sigma)$  as the  $\text{SL}_3$ -skein algebra of the surface  $\Sigma$ .

**Definition 2.3.** We call  the **H-resolution** of the crossings appearing in (3) and (4).

**2.2. Bases of the  $\text{SL}_3$ -skein algebras.** If two web diagrams in a surface  $\Sigma$  represent two isotopic webs in the thickened surface  $\tilde{\Sigma} = \Sigma \times (-1, 1)$ , we will consider them as the same web diagram. We will implicitly identify a web diagram in  $\Sigma$  with the corresponding isotopy class of webs in  $\tilde{\Sigma}$ .



**Lemma 2.4.** [FS22, Page 6] *Any two isotopic crossingless web diagrams differ by a planar isotopy and flip moves (Figure 1).*

**Definition 2.5.** A crossingless web diagram is called **non-elliptic** if it has none of the following elliptic faces:

$$\begin{array}{|c|} \hline \text{---} \circlearrowleft \text{---} \\ \hline \end{array}, \quad \begin{array}{|c|} \hline \text{---} \text{---} \\ \hline \end{array}, \quad \begin{array}{|c|} \hline \text{---} \circlearrowright \text{---} \\ \hline \end{array}, \quad \begin{array}{|c|} \hline \text{---} \text{---} \\ \hline \end{array}, \quad \begin{array}{|c|} \hline \text{---} \text{---} \\ \hline \end{array} \quad (10)$$

By the method of confluence, following [SW07], we obtain the following result.

**Theorem 2.6** ([FS22], Proposition 4). *Let  $\Sigma$  be a marked surface. Then the set of all non-elliptic web diagrams in  $\Sigma$ , denoted by  $B_\Sigma$ , forms an  $R$ -module basis of the skein algebra  $\mathcal{S}(\Sigma)$ .*

**Remark 2.7.** *Compared with our definition of the  $\text{SL}_3$ -skein algebra, the authors of [FS22] introduce an additional relation, namely relation (5) in [FS22], in their definition of the so-called reduced  $\text{SU}_3$ -skein algebra. Consequently, in addition to the elliptic faces listed in (10), their theory excludes one further type of elliptic face, depicted in . As a result, the basis of their reduced  $\text{SU}_3$ -skein algebra consists of crossingless web diagrams without faces of the types appearing in (10) or in ; see [FS22, Proposition 4].*

**2.3. Graded  $\text{SL}_3$ -skein algebras.** Let  $C$  be an oriented closed curve in  $\Sigma$ , and let  $W$  be a crossingless web diagram on  $\Sigma$ . Define  $i(C, W)$  to be the minimal geometric intersection number between  $C$  and  $W$ . We say that  $W$  is in *minimal intersection position* with respect to  $C$  if this minimum is realized.

Assume that  $W$  is in minimal intersection position with respect to  $C$ . Placing  $C$  above  $W$ , we define

$$\begin{aligned} i_1(C, W) &:= \text{the number of positive crossings between } C \text{ and } W, \\ i_2(C, W) &:= \text{the number of negative crossings between } C \text{ and } W. \end{aligned} \quad (11)$$

We will prove that  $i_1(C, W)$  and  $i_2(C, W)$  are well-defined (Proposition 5.5).

Let  $\mathcal{C} = \{C_1, \dots, C_n\}$  be a collection of non-parallel disjoint closed curves in  $\Sigma$ . Define

$$i(\mathcal{C}, W) := \sum_{1 \leq j \leq n} i(C_j, W).$$

For each  $n \in \mathbb{N}$ , define

$$F_{\leq n} := R\text{-span}\{W \in B_\Sigma \mid i(\mathcal{C}, W) < n\}.$$

We define the associated graded algebra

$$\mathcal{S}_\mathcal{C}(\Sigma) := \bigoplus_{n \in \mathbb{N}} F_{\leq n} / F_{\leq n-1}, \quad (12)$$

where we set  $F_{\leq -1} := 0$ .

For any  $W \in \mathcal{S}(\Sigma)$  with  $W \in F_{\leq n} \setminus F_{\leq n-1}$ , we denote by

$$[W] := W + F_{\leq n-1} \in \mathcal{S}_\mathcal{C}(\Sigma)$$

its image in the graded algebra. Proposition 2.6 immediately implies the following result.

**Lemma 2.8.** *The set  $\{[W] \mid W \in B_\Sigma\}$  forms an  $R$ -basis of  $\mathcal{S}_\mathcal{C}(\Sigma)$ .*

### 3. UNBOUNDED $\text{SL}_3$ -LAMINATIONS AND THEIR SHEAR COORDINATES

In this section, we review unbounded  $\text{SL}_3$ -laminations on a punctured surface and their shear coordinates, following [IK25]. These results will be used in §5 and §6. In this section, we will assume that the surface  $\Sigma$  is a punctured surface.

**3.1. Unbounded  $\text{SL}_3$ -laminations.** An *unbounded  $\text{SL}_3$ -lamination* on a punctured surface  $\Sigma$  is an immersed, oriented, uni-trivalent graph  $W$  in  $\bar{\Sigma}$  such that each univalent vertex lies in  $\mathcal{M}$ , while the remaining part of  $W$  is embedded in  $\Sigma$ . Moreover,  $W$  contains none of the elliptic faces listed in (10), nor any of the elliptic faces associated with punctures in  $\mathcal{M}$ , namely

$$\begin{array}{c} \text{[Diagram 1: Circle with a dot at the bottom]} \end{array}, \quad \begin{array}{c} \text{[Diagram 2: Circle with a dot at the bottom and a vertical line segment extending upwards]} \end{array}. \quad (13)$$

We consider unbounded  $\text{SL}_3$ -laminations up to flip moves (Figure 1) and the following equivalence moves:

$$\begin{array}{c} \text{[Diagram 14: Two vertices connected by two curved edges, one above and one below, with arrows pointing towards the vertices]} \end{array} \sim \begin{array}{c} \text{[Diagram 14: Two vertices connected by two curved edges, one above and one below, with arrows pointing away from the vertices]} \end{array}, \quad (14)$$

$$\begin{array}{c} \text{[Diagram 15: A triangle with a dot at the bottom vertex]} \end{array} \sim \begin{array}{c} \text{[Diagram 15: A triangle with a dot at the top vertex]} \end{array}, \quad (15)$$

$$\begin{array}{c} \text{[Diagram 16: A circle with a dot in the center]} \end{array} \sim \begin{array}{c} \text{[Diagram 16: A square with a dot in the center]} \end{array}, \quad (16)$$

$$\begin{array}{c} \text{[Diagram 17: A circle with a dot in the center and several arrows pointing outwards]} \end{array} \sim \begin{array}{c} \text{[Diagram 17: A circle with a dot in the center and several arrows pointing outwards, with a different orientation]} \end{array}, \quad (17)$$

the move obtained by reversing the orientations of the two diagrams in (17). (18)

We use  $\mathcal{L}(\Sigma)$  to denote the set of unbounded  $\mathrm{SL}_3$ -laminations on  $\Sigma$ .

**Remark 3.1.** In [IK25], the authors study signed rational unbounded  $\mathrm{SL}_3$ -laminations, where each endpoint of the underlying uni-trivalent graph is equipped with a sign ‘+’ or ‘-’, and each connected component is labeled by a rational number, modulo the equivalence relations given in [IK25, Definition 2.6].

The space  $\mathcal{L}(\Sigma)$  considered here corresponds to the subspace consisting of  $\mathrm{SL}_3$ -laminations with only ‘+’ signs at their endpoints and integral labels. This restricted setting is sufficient for our purposes and aligns naturally with the framework of the present paper; therefore, we adopt  $\mathcal{L}(\Sigma)$  rather than the more general construction in [IK25].

For each positive integer  $k$ , we use  $\mathbb{D}_k$  to denote the marked surface obtained from a closed disk by removing  $k$  points from its unique boundary component.

To study the unbounded  $\mathrm{SL}_3$ -laminations, we first review the unbounded essential webs in  $\mathbb{D}_2$  and  $\mathbb{D}_3$ .

Let  $E_L$  and  $E_R$  denote the boundary intervals of a biangle  $\mathbb{D}_2$ . A *finite symmetric strand set* on  $\mathbb{D}_2$  is a pair  $S_{\mathbb{D}_2} = (S_L, S_R)$ , where  $S_L$  and  $S_R$  are finite collections of pairwise disjoint oriented strands (i.e. germs of oriented arcs). For each  $Z \in \{L, R\}$ , the strands in  $S_Z$  are located on  $E_Z$ , and the number of incoming (resp. outgoing) strands on  $E_L$  is equal to the number of outgoing (resp. incoming) strands on  $E_R$  (see [IK25, Figure 5]).

Given a symmetric strand set  $S_{\mathbb{D}_2} = (S_L, S_R)$ , the associated *ladder-web*  $W(S)$  on  $\mathbb{D}_2$  is constructed as follows. First, let  $W_{\mathrm{br}}(S)$  denote the unique collection of oriented curves connecting the strands in  $S_L$  to those in  $S_R$  in an order-preserving and minimally intersecting manner. This collection is characterized by a pairing map

$$f_W: S_L \longrightarrow S_R,$$

which is an order-preserving bijection that sends each incoming (resp. outgoing) strand in  $S_L$  to an outgoing (resp. incoming) strand in  $S_R$ . The ladder-web  $W(S)$  is then obtained from  $W_{\mathrm{br}}(S)$  by resolving each crossing using the H-resolution (Definition 2.3).

**Definition 3.2.** [IK25, Definition 3.2] An *asymptotically periodic symmetric strand set*  $S_{\mathbb{D}_2} = (S_L, S_R)$  on  $\mathbb{D}_2$  consists of countable collections  $S_L$  and  $S_R$  of pairwise disjoint oriented strands, where the strands in  $S_Z$  are located on  $E_Z$  and have no accumulation points, for each  $Z \in \{L, R\}$ . The oriented strands are required to be symmetric and periodic outside a compact set; see [IK25, Figure 6].

More precisely, we require that there exists a compact strip  $K \subset \mathbb{D}_2 \setminus \mathcal{M}$  such that:

- $K$  is bounded by two parallel arcs  $\alpha_1$  and  $\alpha_2$ , transverse to the boundary intervals of  $\mathbb{D}_2$ , with  $\alpha_1 \cup \alpha_2$  disjoint from the strand sets  $S_L$  and  $S_R$ ;
- the pair  $(S_L \cap K, S_R \cap K)$  is a finite symmetric strand set;
- the orientation patterns of the strands in  $S_L$  and  $S_R$  lying in  $\mathbb{D}_2 \setminus K$  are periodic, and the pairing map

$$f_K: S_L \cap K \longrightarrow S_R \cap K$$

of the finite symmetric strand set extends to an order-preserving bijection

$$f: S_L \longrightarrow S_R$$

that sends each incoming (resp. outgoing) strand of  $S_L$  to an outgoing (resp. incoming) strand of  $S_R$ .

Unlike the finite case, the pairing map  $f$  need not be unique, as it may depend on the choice of the compact strip  $K$ . Given such a pair  $(S, f)$ , one obtains a collection  $W_{\mathrm{br}}(S, f)$  of oriented curves in mutual minimal position, and the associated ladder-web  $W(S, f)$  is constructed in the same manner as in the finite case. We call  $W(S, f)$  the **ladder-web associated with the pair**  $(S, f)$ . We require that there is no crossing between oriented curves in  $W_{\mathrm{br}}(S, f)$  whose endpoints lie in  $\partial\mathbb{D}_2 \setminus K$ .

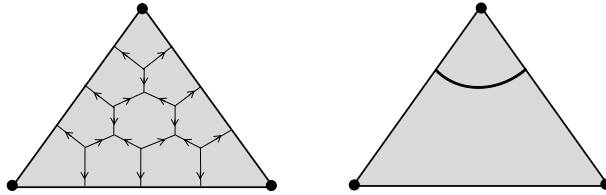


FIGURE 2. The left picture is an example for  $\mathcal{H}_{-3}$  in  $\mathbb{D}_3$ , the right picture is an example for a corner arc in  $\mathbb{D}_3$  (the orientation of the corner arc is arbitrary).



FIGURE 3. Clockwise direction of spiralling.

**Definition 3.3.** [IK25, Definition 3.3] An **unbounded essential web** in  $\mathbb{D}_2$  is an isotopy class of the ladder-web associated with a pair  $(S, f)$  as above.

We now look at webs in  $\mathbb{D}_3$ .

The *honeycomb* of degree  $d$  (with  $d \in \mathbb{Z}$ ), denoted by  $\mathcal{H}_d$ , is a crossingless web in  $\mathbb{D}_3$ . Figure 2 illustrates the honeycomb  $\mathcal{H}_{-3}$ ; reversing the orientation yields  $\mathcal{H}_3$ . By convention,  $\mathcal{H}_0$  is the empty web in  $\mathbb{D}_3$ . We define the *weight* of the honeycomb  $\mathcal{H}_d$  to be  $|d|$ .

An essential web in  $\mathbb{D}_3$  consists of a unique (possibly empty) honeycomb component together with a collection of pairwise disjoint oriented arcs located at the corners of  $\mathbb{D}_3$  (see Figure 2). These oriented arcs are called *corner arcs*. As in the biangle case, we define the following unbounded version.

**Definition 3.4.** [IK25, Definition 3.6] An **unbounded essential web** in  $\mathbb{D}_3$  is the isotopy class of a disjoint union of a (possibly empty) essential web in  $\mathbb{D}_3$  and, at each corner, at most one semi-infinite periodic collection of corner arcs.

To introduce the  $\mathrm{SL}_3$ -shear coordinates, we associate to each unbounded  $\mathrm{SL}_3$ -lamination a spiralling diagram as follows.

**Definition 3.5.** Let  $W$  be an unbounded  $\mathrm{SL}_3$ -lamination on  $\Sigma$ . The associated spiralling diagram  $\widetilde{W}$  is constructed by the following procedure. For each puncture  $p \in \mathcal{M}$ , choose a sufficiently small disk neighborhood  $D_p$  of  $p$  and deform each end of  $W$  incident to  $p$  into an infinitely spiralling curve, spiralling in the clockwise direction, as illustrated in Figure 3.

We say that  $\Sigma$  is **triangulable** if each component of  $\Sigma$  is not a sphere with less than three punctures.

An embedding  $c : (0, 1) \rightarrow \Sigma$  is called an **ideal arc** if both  $\bar{c}(0)$  and  $\bar{c}(1)$  are punctures, where  $\bar{c} : [0, 1] \rightarrow \bar{\Sigma}$  is the ‘closure’ of  $c$ . By an ideal arc we often mean its image in  $\Sigma$ . An **ideal triangulation**, or a **triangulation**  $\Delta$  of  $\Sigma$ , is a collection of mutually disjoint ideal arcs in  $\Sigma$  with the following properties:

- (T1) any two arcs in  $\Delta$  are not isotopic;
- (T2)  $\Delta$  is maximal under condition (T1);
- (T3) the valence of  $\Delta$  at each puncture is at least two.

For each edge  $E$  of  $\Delta$ , we take two disjoint copies  $E'$  and  $E''$  of  $E$  such that no two edges in the collection

$$\bigcup_{E \in \Delta} \{E', E''\}$$

intersect. We define

$$\widehat{\Delta} := \bigcup_{E \in \Delta} \{E', E''\}, \quad (19)$$

and call  $\widehat{\Delta}$  a **split** triangulation of  $\Delta$ . Cutting the surface  $\Sigma$  along the edges of  $\widehat{\Delta}$  yields a collection of bigons and triangles. For each  $E \in e(\Delta)$ , we denote by  $B_E$  the bigon in  $\widehat{\Delta}$  bounded by  $E'$  and  $E''$ , and we denote by  $t(\Delta)$  the set of triangular faces of  $\widehat{\Delta}$ .

**Definition 3.6.** *The spiralling diagram  $\widetilde{W}$  is said to be **in good position** with respect to a split triangulation  $\widehat{\Delta}$  if, for each  $E \in e(\Delta)$  and each  $T \in t(\Delta)$ , both intersections  $\widetilde{W} \cap B_E$  and  $\widetilde{W} \cap T$  are unbounded essential webs.*

Any spiralling diagram arising from an unbounded lamination on  $\Sigma$  can be isotoped into good position with respect to  $\widehat{\Delta}$  [IK25, Theorem 3.10].

**3.2.  $SL_3$ -shear coordinates.** Before introducing the  $SL_3$ -shear coordinates, we first fix some equivalent notations for honeycombs. The following three diagrams all represent a honeycomb of weight  $n$ . Its degree is  $n$  (resp.,  $-n$ ) if the strands incident to the triangle are oriented towards (resp. away from) the triangle:

$$\begin{array}{c} \text{Diagram 1: Triangle with 3 external strands (n) and 3 internal strands} \\ \sim \text{Diagram 2: Triangle with 3 external strands (n) and 1 internal strand (n)} \\ \sim \text{Diagram 3: Triangle with 3 external strands (n) and 2 internal strands (n1, n2)} \end{array} \quad (20)$$

We equip  $\Delta$  with two distinguished points in the interior of each edge and one distinguished point in the interior of each triangle. We denote the set of all such points by  $I(\Delta)$ .

Let  $W \in \mathcal{L}(\Sigma)$  be an  $SL_3$ -lamination. Let  $\widetilde{W}$  denote the associated spiralling diagram, placed in good position with respect to  $\widehat{\Delta}$ . Let  $W_{\text{br}}^{\Delta}$  be its braid representative. The shear coordinates of  $W$  will be defined in terms of  $W_{\text{br}}^{\Delta}$ .

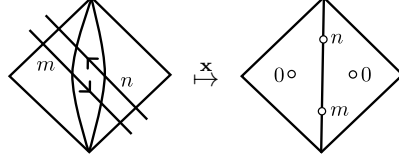
For each  $E \in \Delta$ , let  $Q_E$  be the unique quadrilateral having  $E$  as its diagonal, viewed as the union of two triangles  $T_L$  and  $T_R$  together with the biangle  $B_E$ . The restriction of  $W_{\text{br}}^{\Delta}$  to each of  $T_L$  and  $T_R$  contains at most one honeycomb web, represented by a triangular symbol as in (20). Any strand of the braid representative  $W_{\text{br}}^{\Delta} \cap Q_E$  that is incident to the triangular symbol in  $T_L$  (if it exists) is called a  $T_L$ -strand. Similarly, one defines  $T_R$ -strands. It may happen that a strand is both a  $T_L$ - and a  $T_R$ -strand, in which case it connects the two honeycombs. After removing all  $T_L$ - and  $T_R$ -strands, the remaining diagram consists of a collection of (possibly intersecting) oriented curves, which we call the *curve components*; see Figure 21.

**Definition 3.7.** [IK25, Definition 3.12] *The  $SL_3$ -shear coordinate system*

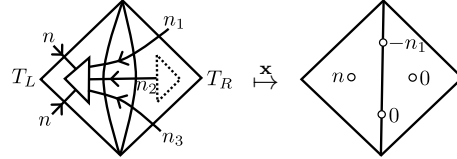
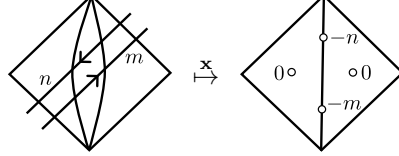
$$\mathbf{x}(W) = (x_i(W))_{i \in I(\Delta)} \in \mathbb{Z}^{I(\Delta)}$$

*is defined as follows. For each edge  $E \in \Delta$ , the coordinates assigned to the four points in the interior of the quadrilateral  $Q_E$  depend only on the restriction  $W_{\text{br}}^{\Delta} \cap Q_E$ .*

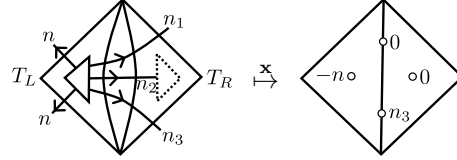
- (1) *Each curve component contributes to the edge coordinates according to the rule illustrated in (21).*
- (2) *The honeycomb in the triangle  $T_L$  contributes to  $\mathbf{x}(W)$  as shown in (22).*
- (3) *The honeycomb in the triangle  $T_R$  and the  $T_R$ -strands contribute symmetrically, via a  $\pi$ -rotation of the configuration in (22).*



(21)



(22)



**Remark 3.8.** The Fock–Goncharov  $p$  map [FG06]  $\mathcal{A} \rightarrow \mathcal{X}$  relates the tropical  $\mathcal{A}$  coordinates in [DS24] and the  $\mathrm{SL}_3$ -shear coordinates by  $p^*(x_i) = \sum_j \varepsilon_{ij} a_j$ . One can also derive the  $\mathrm{SL}_3$ -shear coordinates by  $p$  map and the tropical  $\mathcal{A}$  coordinates from the square case, which is shown in the computation right after [DS25, Definition 4.13] or [DS25, arXiv version 1, Remark 6.4].

It is well-known that [IK25, Theorem 3.19]

$$\mathbf{x}: \mathcal{L}(\Sigma) \rightarrow \mathbb{Z}^{I(\Delta)}, \quad W \mapsto (x_i(W))_{i \in I(\Delta)}$$

is a well-defined injection.

Let  $\Sigma_{0,3}$  denote the third-punctured sphere. Let  $\lambda$  be the unique ideal triangulation of  $\Sigma_{0,3}$ , and label the set  $I(\lambda)$  as in Figure 4. Since the triangulation of  $\Sigma_{0,3}$  is unique, we denote  $I(\lambda)$  by  $I(\Sigma_{0,3})$ . Define

$$\Lambda \subset \mathbb{Z}^{I(\Sigma_{0,3})} := \left\{ \begin{aligned} &x_{11} + x_{32} \geq 0, \quad x_{12} + x_{31} + x_v + x_{v'} \geq 0, \quad x_{31} + x_{22} \geq 0, \\ &x_{32} + x_{21} + x_v + x_{v'} \geq 0, \quad x_{21} + x_{12} \geq 0, \quad x_{22} + x_{11} + x_v + x_{v'} \geq 0 \end{aligned} \right\}. \quad (23)$$

We thank Tsukasa Ishibashi for pointing out the following result, which follows immediately from [IK25, Theorem 3.19] and [IK24, Proposition 4.4].

**Lemma 3.9.** *The coordinate map*

$$\mathbf{x}: \mathcal{L}(\Sigma_{0,3}) \longrightarrow \mathbb{Z}^{I(\Sigma_{0,3})}$$

*is injective, and its image is precisely  $\Lambda$ .*

#### 4. GENERAL POSITIONS OF BASIS ELEMENTS IN PANTS DECOMPOSITIONS OF A CLOSED SURFACE

A pair of pants is a surface homeomorphic to  $S^2$  with three open disks removed.

We use  $P$  to denote a pair of pants, whose three boundary components are labeled by  $C_1, C_2$ , and  $C_3$ . Let  $P'$  be the marked surface obtained from  $P$  by removing one point from each boundary component.

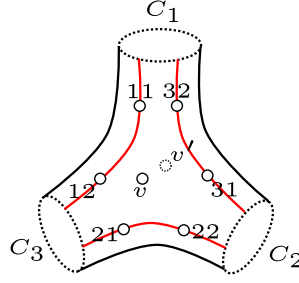


FIGURE 4. We depict  $\Sigma_{0,3}$  as a pair of pants with its boundary removed. The triangulation is given by the three red curves. The set  $I(\Sigma_{0,3})$  is labeled by  $11, 12, 21, 22, 31, 32, v, v'$ , where  $v$  (resp.  $v'$ ) lies in the front (resp. back) triangle. The three punctures of  $\Sigma_{0,3}$  (equivalently, the three boundary components of the pair of pants) are labeled by  $C_1, C_2, C_3$ .

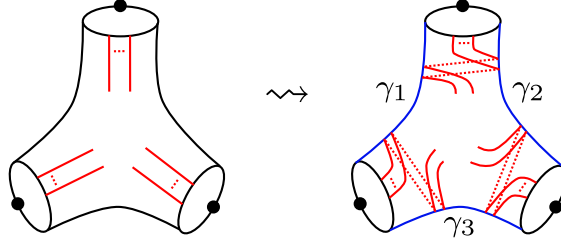


FIGURE 5. The procedure to obtain  $W_1$  from  $W$ .

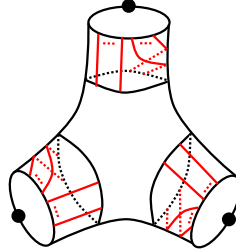


FIGURE 6. The picture for  $W \cap (P' \setminus \tilde{P})$ .

**Definition 4.1.** A non-elliptic web diagram  $W$  in  $P'$  is called **essential** if it can be isotoped so that the following conditions hold.

- (C1) Let  $W_1$  be obtained from  $W$  by performing a full twist along the curves  $C_1, C_2, C_3$  in the direction indicated in Figure 5. Then  $W_1$  is in minimal intersection position with the blue curves  $\gamma_1, \gamma_2$ , and  $\gamma_3$  shown in Figure 5.
- (C2) Let  $C'_1, C'_2, C'_3$  be any closed curves in  $P'$  parallel to  $C_1, C_2, C_3$ , respectively, and suppose that

$$i(C_j, W) = i(C'_j, W), \quad 1 \leq j \leq 3.$$

Note that  $C'_1, C'_2, C'_3$  bound a pair of pants in  $P'$ , which we denote by  $\tilde{P}$ . Then the intersection

$$W \cap (P' \setminus \tilde{P})$$

is as illustrated in Figure 6.

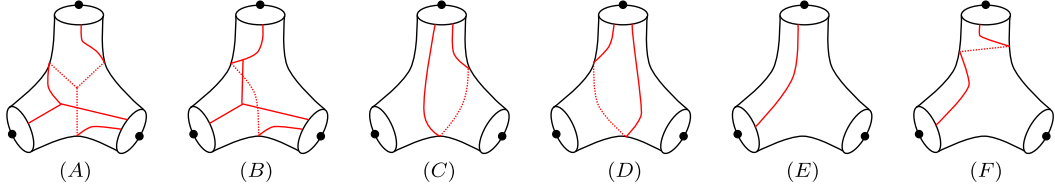


FIGURE 7. The picture for  $W \cap (P' \setminus \tilde{P})$ .

For example, the web diagram in Figure 7(B) does not satisfy (C1), whereas the web diagram in Figure 7(A) is essential. The web diagram in Figure 7(D) satisfies neither (C1) nor (C2), whereas the web diagram in Figure 7(C) is essential. The web diagram in Figure 7(F) does not satisfy (C2), whereas the one shown in Figure 7(E) is essential. One can isotope the web diagram in Figure 7(B) so that it satisfies (C1); however, the resulting diagram fails to satisfy (C2). It is impossible to isotope the web diagrams in Figure 7(D) and (F) so that they satisfy (C2).

Let  $\Sigma_g$  denote a closed surface of genus  $g$ . Throughout this section, we assume that  $g \geq 2$ . Let  $\{C_i\}_{i=1}^{3g-3}$  be a collection of nontrivial simple closed curves on  $\Sigma_g$  that are pairwise non-homotopic; such a collection is called a *pants decomposition* of  $\Sigma_g$ . We call  $\{C_i\}_{i=1}^{3g-3}$  *oriented* if each  $C_i$  is oriented. For each  $i = 1, \dots, 3g-3$ , let  $N(C_i)$  be a small closed annular neighborhood of  $C_i$  in  $\Sigma_g$ . Removing  $\bigsqcup_{i=1}^{3g-3} \text{Int } N(C_i)$  from  $\Sigma_g$  yields a surface that is a disjoint union of pairs of pants.

A *dual graph* is a trivalent graph  $\Gamma$  embedded in  $\Sigma_g$  such that each curve  $C_i$  ( $i = 1, \dots, 3g-3$ ) intersects  $\Gamma$  in exactly one point, and the intersection of  $\Gamma$  with each pair of pants consists of a single trivalent vertex.

Let  $P$  be a pair of pants associated to  $\{C_i\}_{i=1}^{3g-3}$ . We say that  $P$  is bounded by  $C_{i_1}, C_{i_2}, C_{i_3}$ , where  $1 \leq i_1, i_2, i_3 \leq 3g-3$ , if its three boundary components are precisely

$$\{\text{one component of } \partial N(C_{i_1})\} \sqcup \{\text{one component of } \partial N(C_{i_2})\} \sqcup \{\text{one component of } \partial N(C_{i_3})\}.$$

Note that the indices  $i_1, i_2, i_3$  need not be distinct: if some  $i_j$  coincide, then the two boundary components of  $N(C_{i_j})$  appear as two distinct boundary components of  $P$ . By abuse of notation, we will refer to the boundary components of  $P$  simply as  $C_{i_1}, C_{i_2}, C_{i_3}$ .

**Definition 4.2.** A non-elliptic web diagram  $W$  in  $\Sigma_g$  is said to be in **general position** with respect to the pants decomposition  $\{C_i\}_{i=1}^{3g-3}$  if, for each  $1 \leq i \leq 3g-3$ , the following conditions are satisfied:

- (a)  $W$  is in minimal position with respect to  $\partial N(C_i)$ ;
- (b)  $W \cap \partial N(C_i) \subset \partial N(C_i) \setminus \Gamma$ ;
- (c) Let  $P$  be a pair of pants associated to  $\{C_i\}_{i=1}^{3g-3}$ , and let  $P' = P \setminus (\partial P \cap \Gamma)$ . Then  $W \cap P'$  is an essential non-elliptic web diagram in  $P'$  (Definition 4.1).

When the pants decomposition is clear from the context, we will omit the phrase “with respect to the pants decomposition  $\{C_i\}_{i=1}^{3g-3}$ .” Since  $W$  contains only finitely many edges and vertices, it can always be isotoped into general position.

In §5 and 6, we analyze the structure of  $W$  within each annulus and each pair of pants.

## 5. WEBS IN AN ANNULUS

In this section, we classify non-elliptic web diagrams in the annulus (Lemma 5.4). More precisely, we show that there are exactly two types of non-elliptic web diagrams in the annulus. One type is obtained by applying the H-resolution to a strict minimal braid in the annulus (Definition 5.1), while the other type is illustrated in Figure 11.

Based on this classification, we define two twist numbers, denoted by  $t_1$  and  $t_2$ , for non-elliptic web diagrams in the annulus (Definition 5.8). The main result of this section is Theorem 5.10, which

FIGURE 8. An illustration of  $\mathbb{A}'$ .

states that the coordinates defined in Definition 5.8 uniquely determine a non-elliptic web diagram in the annulus up to its signature (see (30)).

The twist numbers introduced here will later be used to define twist numbers for non-elliptic web diagrams in  $\Sigma_g$  ( $g \geq 2$ ), within each annulus associated to a pants decomposition of  $\Sigma_g$ .

**5.1. Braids and braided webs in the annulus.** Let  $\mathbb{A}$  denote the annulus  $S^1 \times [0, 1]$ . We define

$$A_0 := S^1 \times \{0\}, \quad A_1 := S^1 \times \{1\}. \quad (24)$$

For any point  $(x, t) \in \mathbb{A}$ , we call  $t$  the *height* of the point. We say that a point  $(x, t)$  is *higher* than another point  $(x', t')$  if  $t > t'$ .

When drawing the annulus, we adopt the convention that the height increases from left to right; that is, the left (resp. right) boundary component is  $A_0$  (resp.  $A_1$ ).

An *increasing curve* (resp. a *decreasing curve*) in  $\mathbb{A}$  is a properly embedded oriented map  $c: [0, 1] \rightarrow \mathbb{A}$  such that

$$c(t) \in S^1 \times \{t\} \quad (\text{res. } c(t) \in S^1 \times \{1 - t\})$$

for all  $t \in [0, 1]$ .

**Definition 5.1.** A **braid**  $\mathcal{B}$  in  $\mathbb{A}$  is a finite collection of increasing curves, decreasing curves, and oriented properly embedded closed curves  $\{c_1, \dots, c_n\}$  in  $\mathbb{A}$  such that:

- (a) for  $i \neq j$ , the intersection  $c_i \cap c_j$  is a finite set contained in the interior of  $\mathbb{A}$ ;
- (b) any two increasing curves (resp. any two decreasing curves) are disjoint; and
- (c) each closed curve is in minimal intersection position with any  $c_i$ .

We say that  $\mathcal{B}$  is **minimal** if the curves  $c_1, \dots, c_n$  are in minimal intersection position, and **strict** if it contains no closed curves.

We allow  $\mathcal{B}$  to be empty. The empty braid is minimal and strict.

The crossingless web diagram in  $\mathbb{A}$  obtained from a braid  $\mathcal{B}$  by resolving each crossing using the H-resolution (Definition 2.3) is called a *braided web* in  $\mathbb{A}$ , denoted by  $H(\mathcal{B})$ . We call  $\mathcal{B}$  the *braid representative* of  $H(\mathcal{B})$ . Note that a braided web may have different braid representatives.

A braided web in  $\mathbb{A}$  is said to be *minimal* (resp. *strict*) if it has a minimal (resp. strict) braid representative.

Let  $\mathbb{A}'$  be a marked surface obtained from  $\mathbb{A}$  by removing one point from each boundary component. Then the above definitions also apply to  $\mathbb{A}'$ . When depicting  $\mathbb{A}'$ , we will, for simplicity, omit the two marked points shown in Figure 8.

Note that a braided web in  $\mathbb{A}'$  (or  $\mathbb{A}$ ) need not be non-elliptic. The following lemma provides an equivalent characterization for non-ellipticity, together with a necessary condition.

**Lemma 5.2.** Let  $\mathcal{B} = \{c_1, \dots, c_n\}$  be a braid in  $\mathbb{A}'$ . Then:

- (a)  $H(\mathcal{B})$  is non-elliptic if and only if  $H(\mathcal{B})$  contains no 4-gons of the type shown in (10).
- (b) If  $H(\mathcal{B})$  is non-elliptic, then  $\mathcal{B}$  is minimal.

*Proof.* (a) The  $\Rightarrow$  direction follows directly from Definition 2.5. For the  $\Leftarrow$  direction, observe that among the elliptic faces listed in (10), the only ones that can occur in  $H(\mathcal{B})$  are 4-gons. Hence the absence of such 4-gons implies that  $H(\mathcal{B})$  is non-elliptic.

(b) Suppose, for contradiction, that  $\mathcal{B}$  is not minimal. Then  $\mathcal{B}$  contains a bigon. By Definition 5.1(b) and (c), this bigon  $\mathbb{D}$  is formed by one decreasing curve and one increasing curve. We

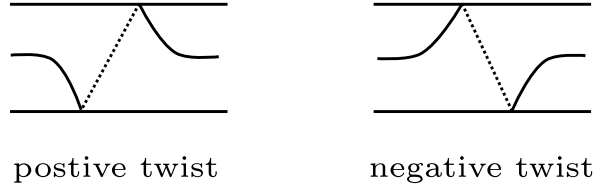


FIGURE 9. The twist number of the left (resp. right) picture is 1 (resp.  $-1$ ).

may assume that  $\mathbb{D}$  contains no smaller bigons in its interior. Let  $b_1$  and  $b_2$  be the two crossings that bound the bigon  $\mathbb{D}$ .

First, assume that no other curves pass through  $\mathbb{D}$ . Then the H-resolutions of  $b_1$  and  $b_2$  produce a 4-gon in  $H(\mathcal{B})$ , contradicting the assumption that  $H(\mathcal{B})$  contains no 4-gons.

Next, suppose that there are curves  $c_{i_1}, \dots, c_{i_m}$  passing through  $\mathbb{D}$ . If some  $c_{i_j}$  is an increasing or decreasing curve, then by Definition 5.1(b) it intersects only one boundary edge of  $\mathbb{D}$ , which would create a smaller bigon inside  $\mathbb{D}$ , contradicting the minimality of  $\mathbb{D}$ . Therefore, all curves  $c_{i_1}, \dots, c_{i_m}$  must be closed curves. By Definition 5.1(c), these closed curves are pairwise disjoint.

If all curves  $c_{i_1}, \dots, c_{i_m}$  have the same orientation, let  $c_{i_j}$  (resp.  $c_{i_k}$ ) be the curve closest to the crossing  $b_1$  (resp.  $b_2$ ). By Definition 5.1(c), the curve  $c_{i_j}$  (resp.  $c_{i_k}$ ) intersects  $\mathbb{D}$  in exactly two points, say  $b_3, b_4$  (resp.  $b_5, b_6$ ). Resolving the crossings  $b_i$  for  $1 \leq i \leq 6$  via the H-resolution produces a 4-gon in  $H(\mathcal{B})$ , again a contradiction.

Now assume that the curves  $c_{i_1}, \dots, c_{i_m}$  do not all have the same orientation. Order them by height, so that  $c_{i_j}$  lies above  $c_{i_k}$  whenever  $j > k$ . If there exists  $2 \leq j \leq m-1$  such that  $c_{i_{j-1}}$  and  $c_{i_{j+1}}$  have the same orientation, while  $c_{i_j}$  has the opposite orientation, then by Definition 5.1(c) the curves  $c_{i_{j-1}}$ ,  $c_{i_j}$ , and  $c_{i_{j+1}}$  intersect  $\mathbb{D}$  in exactly two points each, say  $d_1, d_2, d_3, d_4$ , and  $d_5, d_6$ , respectively. Resolving the crossings  $d_i$  for  $1 \leq i \leq 6$  via the H-resolution again produces a 4-gon in  $H(\mathcal{B})$ , a contradiction.

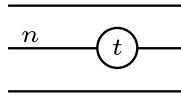
Otherwise, there exists  $1 \leq k \leq m-1$  such that  $c_{i_1}, \dots, c_{i_k}$  have the same orientation, while  $c_{i_{k+1}}, \dots, c_{i_m}$  all have the opposite orientation. By Definition 5.1(c), the curves  $c_{i_1}, c_{i_k}, c_{i_{k+1}}$ , and  $c_{i_m}$  each intersect  $\mathbb{D}$  in exactly two points, say  $e_1, e_2, e_3, e_4, e_5, e_6$ , and  $e_7, e_8$ , respectively. Resolving the crossings  $e_i$ , for  $1 \leq i \leq 8$ ,  $b_1$ , and  $b_2$  via the H-resolution again yields a 4-gon in  $H(\mathcal{B})$ , a contradiction.

These contradictions show that  $\mathcal{B}$  must be minimal.  $\square$

**5.2. Non-elliptic web diagrams in the annulus.** In this subsection, we will classify non-elliptic web diagrams in  $\mathbb{A}$  (Lemma 5.4 and Proposition 5.5). We first introduce some notations.

Let  $c$  be a decreasing or increasing curve in  $\mathbb{A}'$ . We define its *twist number*  $t(c)$  as illustrated in Figure 9.

For  $n \in \mathbb{N}$  and  $t \in \mathbb{Z}$  ( $t = 0$  if  $n = 0$ ), we use the symbol



to denote the diagram obtained from  $n$  parallel strands by introducing twists so that the total twist number is  $t$ ; see Figure 10 for one example.

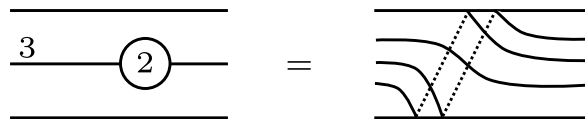


FIGURE 10. One example of twisted parallel strands.



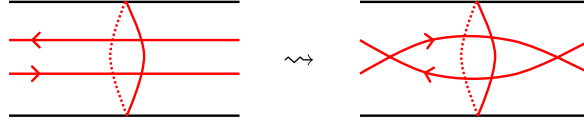


FIGURE 12. A reordering move for curves intersecting a closed curve in  $\mathcal{B}$ . The orientation of the closed curve is arbitrary.

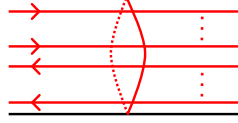


FIGURE 13. The local configuration of  $\mathcal{B}_1$  around each closed curve.

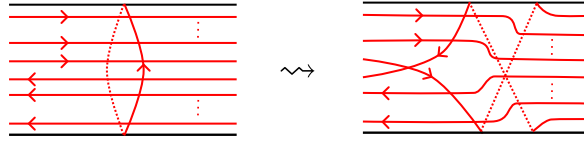


FIGURE 14. A move eliminating closed curves in the braid.

*Proof.* (a) Suppose that  $\mathcal{B}$  is a braid representative of  $W$ . Lemma 5.2(b) implies that  $W$  is minimal.

Assume that  $W$  is not a strict minimal braided web. It then suffices to show that  $W$  is a line-circle web. Note that  $\mathcal{B}$  contains at least one oriented closed curve  $c$  because  $W$  is not a strict minimal braided web.

We first show that  $\mathcal{B}$  cannot contain both increasing and decreasing curves. Suppose, to the contrary, that it does. We will construct a strict minimal braid  $\mathcal{B}'$  such that  $H(\mathcal{B}') = W$ .

Let  $C$  be a closed curve in  $\mathbb{A}'$  parallel to a boundary component. Recall the graded algebra  $\mathcal{S}_C(\mathbb{A}')$  defined in §2.3. It is straightforward to check that the two braids shown in Figure 12 represent the same element of  $\mathcal{S}_C(\mathbb{A}')$ . By repeatedly applying the move in Figure 12 to  $\mathcal{B}$ , we obtain a new braid  $\mathcal{B}_1$  such that

$$[H(\mathcal{B})] = [H(\mathcal{B}_1)] \in \mathcal{S}_C(\mathbb{A}'),$$

and such that the local configuration of  $\mathcal{B}_1$  around each closed curve is as in Figure 13.

Next, note that the two braids in Figure 14 (resp. Figure 15) represent the same element of  $\mathcal{S}(\mathbb{A}')$ . Applying the moves in Figures 14 and 15 to each closed curve in  $\mathcal{B}_1$ , we obtain a new braid  $\mathcal{B}_2$  such that

$$H(\mathcal{B}_1) = H(\mathcal{B}_2) \in \mathcal{S}(\mathbb{A}'),$$

and  $\mathcal{B}_2$  is strict. Let  $\mathcal{B}'$  be the minimal strict braid obtained from  $\mathcal{B}_2$  by removing all bigons. Then

$$[W] = [H(\mathcal{B})] = [H(\mathcal{B}_1)] = [H(\mathcal{B}_2)] = [H(\mathcal{B}')] \in \mathcal{S}_C(\Sigma).$$

By Lemma 2.8, this implies that  $W = H(\mathcal{B}')$ , contradicting the assumption that  $W$  is not a strict minimal braided web.

Therefore,  $\mathcal{B}$  cannot contain both increasing and decreasing curves. The claim now follows from Lemma 5.3.

(b) Suppose that  $W = H(\mathcal{B}) = H(\mathcal{B}')$  for two strict minimal braids  $\mathcal{B}$  and  $\mathcal{B}'$ . Lemma 2.4 implies that  $H(\mathcal{B})$  and  $H(\mathcal{B}')$  differ by a planar isotopy. Consequently,  $\mathcal{B}$  and  $\mathcal{B}'$  themselves are related by a planar isotopy, and hence  $\mathcal{B} = \mathcal{B}'$ .  $\square$

The following shows that any non-elliptic web in  $\mathbb{A}$  is in fact a non-elliptic braided web. This guarantees that the twist numbers defined in Definition 5.8 can be used to define twist numbers

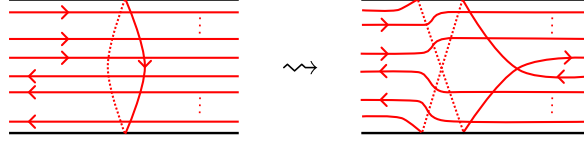


FIGURE 15. Another move eliminating closed curves in the braid.

for non-elliptic web diagrams on  $\Sigma_g$ , associated to each annulus in a pants decomposition of  $\Sigma_g$ . Moreover, this allows us to apply Theorem 5.10 to non-elliptic web diagrams on  $\Sigma_g$ , annulus by annulus, with respect to a pants decomposition of  $\Sigma_g$ .

**Proposition 5.5.** *Let  $\Sigma$  be a marked surface, let  $W$  be a crossingless web diagram in  $\Sigma$ , and let  $\mathbb{A}$  be an embedded annulus in  $\Sigma$  with boundary components  $C_1$  and  $C_2$ . Suppose that  $W$  is in minimal intersection position with respect to  $C_1$  and  $C_2$ . Then:*

- (a) *If  $W \cap \mathbb{A}$  contains no trivial loops, 2-gons, or 4-gons in (10), the web  $W \cap \mathbb{A}$  is a non-elliptic braided web.*
- (b) *If  $C_1$  and  $C_2$  are oriented in the same direction, then*

$$i_1(C_1, W) = i_1(C_2, W) \quad \text{and} \quad i_2(C_1, W) = i_2(C_2, W) \quad (\text{see (11)}). \quad (29)$$

*Proof.* (a) Set  $W' := W \cap \mathbb{A}$ . We regard  $\mathbb{A}$  as the twice-punctured sphere  $\Sigma_{0,2}$  by viewing the two boundary components of  $\mathbb{A}$  as punctures. Then  $W'$  is an unbounded lamination in  $\Sigma_{0,2}$ , since  $W$  is in minimal intersection position with respect to  $\partial\mathbb{A}$ . Let  $\mathcal{W}$  be the spiralling diagram of  $W'$  (Definition 3.5). By [IK25, Proposition 6.4 and Lemma 6.5], there exists an ideal arc  $E$  in  $\Sigma_{0,2}$  such that, after cutting  $\mathcal{W}$  along  $E$ , we obtain an unbounded essential web  $\mathcal{W}'$  in the bigon  $\mathbb{D}_2$  (Definition 3.3).

Let  $K$  be a compact strip from Definition 3.2. We label the oriented strands in  $S_L$  (resp.  $S_R$ ) by  $l_i$  (resp.  $r_i$ ),  $i \in \mathbb{Z}$ , so that  $K \cap S_L = \{l_1, \dots, l_k\}$  and  $K \cap S_R = \{r_1, \dots, r_k\}$ . There exists an identification  $F: E_L \rightarrow E_R$  such that  $F(l_i) = r_{i+m}$  for some integer  $m$ , and

$$\Sigma_{0,2} = \mathbb{D}_2 / (F(x) = x, x \in E_L), \quad \mathcal{W} = \mathcal{W}' / (l_i = r_{i+m}, i \in \mathbb{Z}).$$

We assume  $m \geq 0$ , since a similar argument applies when  $m < 0$ . Let  $E'_L$  (resp.  $E'_R$ ) be a closed subinterval of  $E_L$  (resp.  $E_R$ ) such that

$$E'_L \cap S_L = \{l_{-m+1}, \dots, l_0, l_1, \dots, l_k\}, \quad E'_R \cap S_R = \{r_1, \dots, r_k, r_{k+1}, \dots, r_{k+m}\}.$$

We may assume that  $F(E'_L) = E'_R$ , since otherwise  $F$  is isotopic to an identification with this property. Let  $\mathcal{W}''$  be the subweb of  $\mathcal{W}'$  consisting of components whose endpoints lie in  $E'_L \sqcup E'_R$ . Let  $\mathcal{B}$  be the braid representative of  $\mathcal{W}''$ .

Define

$$\mathbb{A}' = \mathbb{D}_2 / (F(x) = x, x \in E'_L), \quad \overline{\mathcal{W}} = \mathcal{W}'' / (l_i = r_{i+m}, -m+1 \leq i \leq k),$$

and

$$\overline{\mathcal{B}} = \mathcal{B} / (l_i = r_{i+m}, -m+1 \leq i \leq k).$$

Then  $\mathbb{A}'$  is obtained from  $\mathbb{A}$  by removing one point from each boundary component. Viewed as a web diagram in  $\mathbb{A}$  via the embedding  $\mathbb{A}' \subset \mathbb{A}$ , the web  $\overline{\mathcal{W}}$  differs from  $W'$  by a sequence of twists of the endpoints of  $W$  along  $A_0$  or  $A_1$  (see (24)). Moreover,  $\overline{\mathcal{B}} \subset \mathbb{A}' \subset \mathbb{A}$  is a braid in  $\mathbb{A}$  because the strands in  $\mathcal{B}$  with the same direction do not intersect each other. We also have  $H(\overline{\mathcal{B}}) = \overline{\mathcal{W}}$ . Hence  $\overline{\mathcal{W}}$  is a braided web, and therefore so is  $W'$ . Lemma 5.2(a) shows that  $W'$  is a non-elliptic braided web.

(b) follows from (a), because removing trivial loops, 2-gons, or 4-gons (Figure 16) in  $W \cap \mathbb{A}$  does not affect the intersection numbers in (29).  $\square$

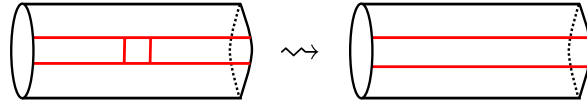


FIGURE 16. The procedure to remove 4-gons in the annulus.

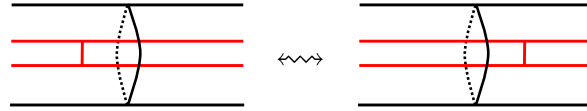


FIGURE 17. The crossbar move.

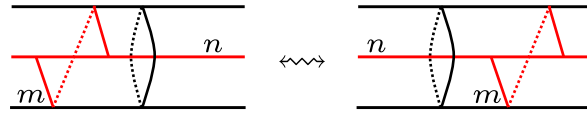


FIGURE 18. The annulus-H move.

Using the technique of [FS22, Proposition 13], we obtain the following corollary from Lemma 2.4 and Proposition 5.5.

**Corollary 5.6.** *Let  $\Sigma$  be a marked surface. The minimal position of any non-elliptic web diagram with respect to any disjoint collection of closed curves  $C_1, \dots, C_n$  in  $\Sigma$  is unique up to crossbar moves (Figure 17), annulus-H moves (Figure 18), twists along some of these closed curves, flip moves (Figure 1), and planar isotopy within the complement of these curves.*

*Proof.* **Step 1: The case  $n = 1$ .** This follows immediately from Lemma 2.4, Proposition 5.5(a), and Lemma 5.4(a).

**Step 2: The general case.** We argue by induction on  $n$ . Let  $C_1, \dots, C_{n+1}$  be  $n + 1$  disjoint closed curves in  $\Sigma$ , and let  $W$  and  $W'$  be two isotopic non-elliptic web diagrams that are both in minimal position with respect to  $C_1, \dots, C_{n+1}$ . By Step 1, the webs  $W$  and  $W'$  can be made isotopic in  $\Sigma \setminus C_{n+1}$  using crossbar moves, annulus-H moves, twists along  $C_{n+1}$ , and flip moves. The desired conclusion then follows from the inductive hypothesis.  $\square$

Definition 4.2 and Corollary 5.6 together imply the following result, which will be used in §7 to define coordinates for non-elliptic web diagrams on a closed surface.

**Corollary 5.7.** *Let  $\mathcal{P}$  be a pants decomposition of  $\Sigma_g$  with  $g \geq 2$ . A non-elliptic web diagram  $W$  in general position with respect to  $\mathcal{P}$  is unique up to crossbar path moves (Figure 19) and flip moves (Figure 1).*

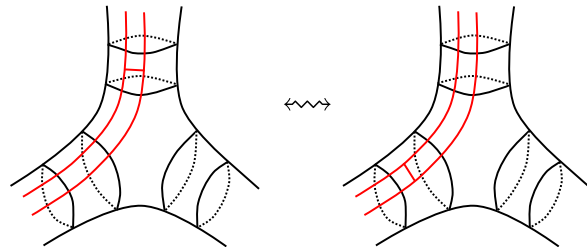


FIGURE 19. The crossbar path move.

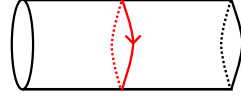


FIGURE 20. The oriented red closed curve is  $C$  (the positive orientation of  $[0, 1]$  is from left to right).

**5.3. Twist numbers.** In this subsection, we will define the coordinates of non-elliptic braided webs in  $\mathbb{A}'$ .

Let  $\mathcal{B} = \{c_1, \dots, c_n\}$  be a strict braid in  $\mathbb{A}'$ . We define

$$\begin{aligned} n_1(\mathcal{B}) &:= \text{the number of increasing curves in } \mathcal{B}, \\ n_2(\mathcal{B}) &:= \text{the number of decreasing curves in } \mathcal{B}, \\ t_1(\mathcal{B}) &:= \sum_{c_i \text{ increasing in } \mathcal{B}} t(c_i), \\ t_2(\mathcal{B}) &:= \sum_{c_i \text{ decreasing in } \mathcal{B}} t(c_i), \end{aligned}$$

where the twist number  $t(c_i)$  is defined as in Figure 9.

**Definition 5.8.** Let  $W$  be a non-elliptic braided web in  $\mathbb{A}'$ . Lemma 5.4(a) implies that  $W$  is either a strict minimal braided web or a line-circle web. We define

$$\mathbf{t}(W) = (n_1(W), n_2(W), t_1(W), t_2(W))$$

as follows:

- If  $W$  is a line-circle web as illustrated in the left picture in Figure 11, define

$$\mathbf{t}(W) := (n, 0, t, m).$$

- If  $W$  is a line-circle web as illustrated in the right picture in Figure 11, define

$$\mathbf{t}(W) := (0, n, m, t).$$

- If  $W$  is a strict minimal braided web represented by a strict minimal braid  $\mathcal{B}$ , define

$$\mathbf{t}(W) := (n_1(\mathcal{B}), n_2(\mathcal{B}), t_1(\mathcal{B}), t_2(\mathcal{B})).$$

Lemma 5.4(b) implies the following result.

**Lemma 5.9.** Let  $W$  be a non-elliptic braided web in  $\mathbb{A}'$ . Then  $\mathbf{t}(W)$  is well defined.

Let  $C = S^1 \times \{\frac{1}{2}\}$ . We orient  $C$  as illustrated in Figure 20. It is straightforward to check that

$$n_1(W) = i_1(C, W), \quad n_2(W) = i_2(C, W).$$

We orient  $A_0, A_1$  (see (24)) in the same direction as  $C$ .

Let  $W$  be a braided web in  $\mathbb{A}'$ , and suppose that

$$W \cap \partial A_0 = \{a_1, \dots, a_n\}, \quad W \cap \partial A_1 = \{a_{n+1}, \dots, a_{2n}\}.$$

Assume that the points  $a_1, \dots, a_n$  (resp.  $a_{n+1}, \dots, a_{2n}$ ) are encountered consecutively when traversing  $A_0$  (resp.  $A_1$ ) in its orientation, starting from the unique puncture in  $A_0$  (resp.  $A_1$ ).

For each  $1 \leq i \leq 2n$ , define a map

$$s: \{a_1, \dots, a_{2n}\} \longrightarrow \{-, +\}$$

by

$$s(a_i) = \begin{cases} + & \text{if the strand incident to } a_i \text{ is increasing,} \\ - & \text{if the strand incident to } a_i \text{ is decreasing.} \end{cases}$$

We call the tuple

$$\mathbf{s}(W) = (s(a_1), \dots, s(a_{2n})) \quad (30)$$

the *signature* of  $W$ .

The following theorem is the main result of this section. It shows that a non-elliptic braided web in  $\mathbb{A}'$  is uniquely determined by its coordinates, as defined in Definition 5.8, together with its signature.

**Theorem 5.10.** *Let  $W$  be a non-elliptic braided web in  $\mathbb{A}'$ . Then  $W$  is uniquely determined by its coordinate*

$$\mathbf{t}(W) = (n_1, n_2, t_1, t_2)$$

together with its signature. Moreover, we have

$$\text{Im } \mathbf{t} = \{(n_1, n_2, t_1, t_2) \in \mathbb{N}^2 \times \mathbb{Z}^2 \mid t_i \geq 0 \text{ if } n_i = 0, \text{ for } i = 1, 2\}.$$

*Proof.* Lemma 5.4(a) implies that  $W$  is either a strict minimal braided web or a line-circle web. It follows immediately that

$$\text{Im } \mathbf{t} = \{(n_1, n_2, t_1, t_2) \in \mathbb{N}^2 \times \mathbb{Z}^2 \mid t_i \geq 0 \text{ if } n_i = 0, i = 1, 2\}.$$

Moreover, it is straightforward to see that

$$\mathbf{t}(W_1) \neq \mathbf{t}(W_2)$$

whenever  $W_1$  is a strict minimal braided web and  $W_2$  is a line-circle web, or when  $W_1 \neq W_2$  are both line-circle webs.

Suppose that  $W$  is a strict minimal braided web, represented by a strict minimal braid  $\mathcal{B}$ . The signature of  $W$ , together with the data  $(n_1, t_1)$  (resp.  $(n_2, t_2)$ ), uniquely determines the increasing (resp. decreasing) curves in  $\mathcal{B}$ . The minimality of  $\mathcal{B}$  then uniquely determines  $\mathcal{B}$ . Hence  $W$  is uniquely determined.  $\square$

## 6. WEBS IN A PAIR OF PANTS

Recall that  $P'$  is the marked surface obtained from the pair of pants  $P$  by removing one point from each boundary component. In this section, we define coordinates for essential non-elliptic web diagrams (Definition 4.1) in the pair of pants  $P'$ ; see Definition 6.1. The main result of this section is Theorem 6.3, which asserts that a non-elliptic web diagram in  $P'$ , up to the moves shown in Figure 22, is uniquely determined by its coordinates.

Let  $W$  be an essential non-elliptic web diagram in  $P'$ . Via the natural embedding  $P' \hookrightarrow P$ , we regard  $W$  as a web diagram in  $P$ . We identify  $P$  with  $\Sigma_{0,3}$  as in Figure 4. By Definition 4.1, it follows that  $W \in \mathcal{L}(\Sigma_{0,3})$ .

We label  $I(\Sigma_{0,3})$  as in Figure 4. Suppose that

$$\mathbf{x}(W) = (x_{11}, x_{12}, x_{21}, x_{22}, x_{31}, x_{32}, x_v, x_{v'}) \in \mathbb{Z}^{I(\Sigma_{0,3})}.$$

We introduce the following coordinates associated to  $W$ .

**Definition 6.1.** *Let  $\overline{B}$  denote the set of essential non-elliptic web diagrams in  $P'$ . Define*

$$\mathbf{P}: \overline{B} \rightarrow \mathbb{Z}^{I(\Sigma_{0,3})}, \quad W \mapsto (n_{11}(W), n_{12}(W), n_{21}(W), n_{22}(W), n_{31}(W), n_{32}(W), t_P(W), h_P(W)),$$

where

$$\begin{aligned}
n_{11}(W) &= x_{11} + x_{32}, \\
n_{12}(W) &= x_{12} + x_{31} + x_v + x_{v'}, \\
n_{21}(W) &= x_{31} + x_{22}, \\
n_{22}(W) &= x_{32} + x_{21} + x_v + x_{v'}, \\
n_{31}(W) &= x_{21} + x_{12}, \\
n_{32}(W) &= x_{22} + x_{11} + x_v + x_{v'}, \\
t_P(W) &= x_v - x_{v'}, \\
h_P(W) &= x_{11} - x_{12} + x_{21} - x_{22} + x_{31} - x_{32}.
\end{aligned} \tag{31}$$

Label the three boundary components of  $P'$  by  $C_1, C_2, C_3$  as in Figure 4. For  $t = 1, 2, 3$ , define the intersection numbers

$$\begin{aligned}
i_{t1}(W) &:= \text{the number of endpoints of } W \text{ on } C_t \text{ pointing towards } C_t, \\
i_{t2}(W) &:= \text{the number of endpoints of } W \text{ on } C_t \text{ pointing away from } C_t.
\end{aligned} \tag{32}$$

The following provides a geometric interpretation of the coordinates  $n_{t1}(W), n_{t2}(W)$ , for  $t = 1, 2, 3$ , in (31); namely, they coincide with the intersection numbers defined in (32).

**Proposition 6.2.** *Let  $W$  be an essential non-elliptic web diagram in  $P'$ . Then, for  $t = 1, 2, 3$ , we have*

$$i_{t1}(W) = n_{t1}(W), \quad i_{t2}(W) = n_{t2}(W).$$

*Proof.* In this proof, we identify the pair of pants  $P$  with  $\Sigma_{0,3}$  and regard  $W$  as an unbounded  $\text{SL}_3$ -lamination on  $\Sigma_{0,3}$ . Let  $\widetilde{W}$  denote the associated spiralling diagram of  $W$  in good position with respect to  $\widehat{\lambda}$ , and let  $W_{\text{br}}$  be its braid representative.

As discussed in [IK24, §4.1], the braid  $W_{\text{br}}$  admits a decomposition

$$W_{\text{br}} = \bigcup_{\alpha} W_{\alpha},$$

where each  $W_{\alpha}$  is connected and consists only of honeycombs of height one. We refer to each web  $W_{\alpha}$  appearing in this decomposition as an *elementary braid* in  $\Sigma_{0,3}$ .

By [IK24, Lemma 4.1], we have

$$n_{t1}(W) = \sum_{\alpha} n_{t1}(W_{\alpha}), \quad n_{t2}(W) = \sum_{\alpha} n_{t2}(W_{\alpha}), \quad t = 1, 2, 3.$$

On the other hand, it is clear that

$$i_{t1}(W) = \sum_{\alpha} i_{t1}(W_{\alpha}), \quad i_{t2}(W) = \sum_{\alpha} i_{t2}(W_{\alpha}), \quad t = 1, 2, 3.$$

Therefore, it suffices to prove the claim when  $W$  is an elementary braid in  $\Sigma_{0,3}$ .

Let  $p$  be a puncture of  $\Sigma_{0,3}$ , corresponding to the boundary component  $C_i$  for some  $i = 1, 2, 3$ . Let  $D^*(p)$  (see Figure 21) be the once punctured bigon obtained by cutting along the other two punctures. Since both  $n_{tj}(W)$  and  $i_{tj}(W)$  ( $j = 1, 2$ ) depend only on the restriction of  $\widetilde{W}$  to  $D^*(p)$ , which contains the puncture  $p$  together with two punctures on its boundary, it suffices to consider the diagram

$$\widetilde{W}_p := \widetilde{W} \cap D^*(p).$$

In [IK24, Figure 10], all possible local configurations of  $\widetilde{W}_p$  are listed. Among the ten pictures in [IK24, Figure 10], our situation corresponds to the seven cases in which the spiralling diagram around the puncture  $p$  is clockwise. A direct inspection of these seven cases shows that

$$n_{tj}(W) = i_{tj}(W) \quad \text{for all } t = 1, 2, 3 \text{ and } j = 1, 2.$$

□

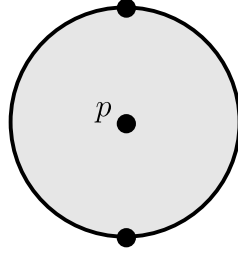
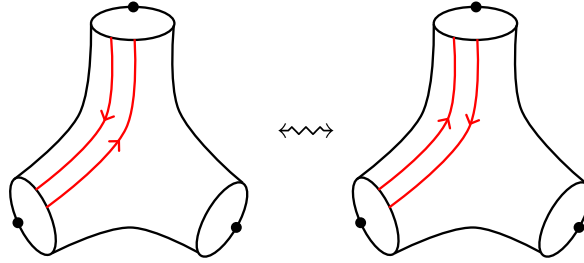
FIGURE 21. Illustration for the once punctured bigon  $D^*(p)$ .

FIGURE 22. The flip move in the pair of pants.

We are now ready to state the main theorem in this section.

**Theorem 6.3.** (a) Let  $W$  and  $W'$  be two essential non-elliptic web diagrams in  $P'$  with  $\mathbf{P}(W) = \mathbf{P}(W')$ . Then  $W$  can be obtained from  $W'$  by a sequence of moves shown in Figure 22, together with the moves obtained by rotating the pictures in Figure 22 by  $120^\circ$  and  $240^\circ$ .

(b) The image  $\text{Im } \mathbf{P}$  consists of all tuples

$$(n_{11}, n_{12}, n_{21}, n_{22}, n_{31}, n_{32}, t_P, h_P) \in \mathbb{Z}^{I(\Sigma_{0,3})}$$

satisfying the following conditions:

$$\begin{cases} n_{11} \geq 0, n_{12} \geq 0, n_{21} \geq 0, n_{22} \geq 0, n_{31} \geq 0, n_{32} \geq 0, \\ n_{12} + n_{22} + n_{32} \equiv n_{11} + n_{21} + n_{31} \pmod{3}, \\ h_P + n_{11} + n_{21} + n_{31} \equiv 0 \pmod{2}, \\ h_P \equiv n_{11} - n_{12} - n_{21} + n_{22} \pmod{3}, \\ 3t_P \equiv n_{12} + n_{22} + n_{32} - n_{11} - n_{21} - n_{31} \pmod{6}. \end{cases} \quad (33)$$

*Proof.* Observe that the equations in (31) are linearly independent. Their inverse transformation is given by

$$\begin{aligned} x_{11} &= \frac{h_P + 3n_{11} - n_{21} - 2n_{22} + n_{31} + 2n_{32}}{6}, \\ x_{12} &= \frac{-h_P + n_{11} + 2n_{12} - n_{21} - 2n_{22} + 3n_{31}}{6}, \\ x_{21} &= \frac{h_P - n_{11} - 2n_{12} + n_{21} + 2n_{22} + 3n_{31}}{6}, \\ x_{22} &= \frac{-h_P - n_{11} - 2n_{12} + 3n_{21} + n_{31} + 2n_{32}}{6}, \end{aligned}$$

$$\begin{aligned}
x_{31} &= \frac{h_P + n_{11} + 2n_{12} + 3n_{21} - n_{31} - 2n_{32}}{6}, \\
x_{32} &= \frac{-h_P + 3n_{11} + n_{21} + 2n_{22} - n_{31} - 2n_{32}}{6}, \\
x_v &= \frac{3t_P - n_{11} + n_{12} - n_{21} + n_{22} - n_{31} + n_{32}}{6}, \\
x_{v'} &= \frac{-3t_P - n_{11} + n_{12} - n_{21} + n_{22} - n_{31} + n_{32}}{6}.
\end{aligned} \tag{34}$$

Part (a) follows directly from Lemma 3.9.

For part (b), using the equations in (31) together with Lemma 3.9, one readily checks that any element

$$(n_{11}, n_{12}, n_{21}, n_{22}, n_{31}, n_{32}, t_P, h_P) \in \text{Im } \mathbf{P}$$

satisfies the relations in (33).

Conversely, let  $(n_{11}, n_{12}, n_{21}, n_{22}, n_{31}, n_{32}, t_P, h_P) \in \mathbb{Z}^{I(\Sigma_{0,3})}$  satisfy (33). Define

$$(x_{11}, x_{12}, x_{21}, x_{22}, x_{31}, x_{32}, x_v, x_{v'}) \in \mathbb{Q}^{I(\Sigma_{0,3})}$$

by the formulas in (34). It is straightforward to verify that

$$(x_{11}, x_{12}, x_{21}, x_{22}, x_{31}, x_{32}, t_v, t_{v'}) \in \Lambda$$

(see (23)). By Lemma 3.9, there exists  $W \in \overline{B}$  such that

$$\mathbf{x}(W) = (x_{11}, x_{12}, x_{21}, x_{22}, x_{31}, x_{32}, x_v, x_{v'}).$$

Applying  $\mathbf{P}$ , we obtain

$$\mathbf{P}(W) = (n_{11}, n_{12}, n_{21}, n_{22}, n_{31}, n_{32}, t_P, h_P),$$

which completes the proof.  $\square$

**Remark 6.4.** *Note that the congruence*

$$n_{12} + n_{22} + n_{32} \equiv n_{11} + n_{21} + n_{31} \pmod{3}$$

*implies*

$$n_{11} - n_{12} - n_{21} + n_{22} \equiv n_{21} - n_{22} - n_{31} + n_{32} \equiv n_{31} - n_{32} - n_{11} + n_{12} \pmod{3}.$$

*Consequently, condition (33) is invariant under the cyclic permutation*

$$n_{1j} \mapsto n_{2j} \mapsto n_{3j} \mapsto n_{1j}.$$

## 7. COORDINATES FOR NON-ELLIPTIC $\text{SL}_3$ WEB DIAGRAMS ON CLOSED SURFACES

In this section, we use the results developed in §5 and §6 to construct coordinates for non-elliptic web diagrams on a closed surface  $\Sigma_g$ . We divide the construction into two cases: the case  $g \geq 2$  (Definition 7.1) and the case  $g = 1$  (Definition 7.5). We then prove that these coordinates uniquely determine a non-elliptic web diagram (Theorems 7.4 and 7.7), which constitute the main results of this paper. As a consequence, we obtain a parametrization of the non-elliptic basis elements of  $\mathcal{S}(\Sigma_g)$ .

**7.1. The genus is more than one.** Let  $\mathcal{P} = \{C_j\}_{1 \leq j \leq 3g-3}$  be an oriented pants decomposition of  $\Sigma_g$  ( $g \geq 2$ ) with dual graph  $\Gamma$ , and let  $W \in B_\Sigma$  be a non-elliptic web diagram in  $\Sigma_g$  in general position with respect to  $\{C_j\}_{1 \leq j \leq 3g-3}$ . We write  $r = 3g - 3$ , let  $\mathbb{P}$  denote the set of pairs of pants determined by  $\{C_j\}_{1 \leq j \leq 3g-3}$ , and for each  $j$  let

$$\mathcal{N}_j := N(C_j) \setminus (\partial N(C_j) \cap \Gamma).$$

We identify each  $\mathcal{N}_j$  with  $\mathbb{A}^1$  so that  $C_j$  is identified with the curve  $C$  in Figure 20, preserving the orientation.

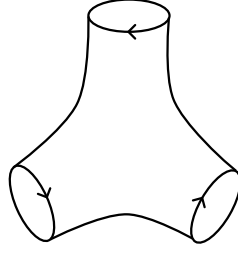


FIGURE 23. The clockwise orientation of the three boundary components of the pair of pants.

**Definition 7.1.** We define the coordinate of  $W$  (with respect to  $\mathcal{P}$ ) by

$$\kappa(W) = \left( (n_{j1}(W))_{1 \leq j \leq r}, (n_{j2}(W))_{1 \leq j \leq r}, (t_{j1}(W))_{1 \leq j \leq r}, (t_{j2}(W))_{1 \leq j \leq r}, (t_P(W))_{P \in \mathbb{P}}, (h_P(W))_{P \in \mathbb{P}} \right),$$

where

$$\begin{aligned} n_{j1}(W) &= i_1(C_j, W) \quad (\text{see (11)}, \text{ for } 1 \leq j \leq r, \\ n_{j2}(W) &= i_2(C_j, W) \quad (\text{see (11)}, \text{ for } 1 \leq j \leq r, \\ t_{j1}(W) &= t_1(\mathcal{N}_j \cap W) \quad (\text{see Definition 5.8}), \text{ for } 1 \leq j \leq r, \\ t_{j2}(W) &= t_2(\mathcal{N}_j \cap W) \quad (\text{see Definition 5.8}), \text{ for } 1 \leq j \leq r, \\ t_P(W) &= t_P(P \cap W) \quad (\text{see Definition 6.1}), \text{ for } P \in \mathbb{P}, \\ h_P(W) &= h_P(P \cap W) \quad (\text{see Definition 6.1}), \text{ for } P \in \mathbb{P}. \end{aligned}$$

We have the following.

**Lemma 7.2.** The coordinates defined in Definition 7.1 are well defined.

*Proof.* The well-definedness of  $t_P$ ,  $h_P$ ,  $t_{i1}$ , and  $t_{i2}$ , follows from Corollary 5.7. The well-definedness of  $n_{i1}$  and  $n_{i2}$  follows from Proposition 5.5(b).  $\square$

Define

$$K := \mathbb{N}^r \times \mathbb{N}^r \times \mathbb{Z}^r \times \mathbb{Z}^r \times \mathbb{Z}^{\mathbb{P}} \times \mathbb{Z}^{\mathbb{P}}.$$

Let

$$\left( (n_{i1})_{1 \leq i \leq r}, (n_{i2})_{1 \leq i \leq r}, (t_{i1})_{1 \leq i \leq r}, (t_{i2})_{1 \leq i \leq r}, (t_P)_{P \in \mathbb{P}}, (h_P)_{P \in \mathbb{P}} \right) \in K.$$

We use Figure 23 to illustrate the clockwise orientation of the three boundary components of the pair of pants. The counterclockwise orientation is defined to be the opposite one.

For each  $P \in \mathbb{P}$ , suppose that  $P$  is bounded by the curves  $C_j$ ,  $C_k$ , and  $C_m$ . We identify  $P$  with the pair of pants in Figure 4 so that  $C_j$ ,  $C_k$ , and  $C_m$  correspond to  $C_1$ ,  $C_2$ , and  $C_3$  in Figure 4, respectively. For a boundary component of  $P$ , if  $C_j$  (resp.  $C_k$  or  $C_m$ ) is oriented counterclockwise (resp. clockwise), we define

$$\begin{aligned} n_{11}^P &= n_{j1}, & n_{12}^P &= n_{j2} & (\text{resp. } n_{11}^P &= n_{j2}, n_{12}^P &= n_{j1}), \\ n_{21}^P &= n_{k1}, & n_{22}^P &= n_{k2} & (\text{resp. } n_{21}^P &= n_{k2}, n_{22}^P &= n_{k1}), \\ n_{31}^P &= n_{m1}, & n_{32}^P &= n_{m2} & (\text{resp. } n_{31}^P &= n_{m2}, n_{32}^P &= n_{m1}). \end{aligned} \tag{35}$$

Although the quantities  $n_{1t}^P, n_{2t}^P, n_{3t}^P$  for  $t = 1, 2$  are not individually well defined, they are well defined up to the cyclic permutation

$$n_{1t} \mapsto n_{2t} \mapsto n_{3t} \mapsto n_{1t}.$$

**Definition 7.3.** Define the submonoid  $\Theta \subset K$  to be the set of all

$$\left( (n_{i1})_{1 \leq i \leq r}, (n_{i2})_{1 \leq i \leq r}, (t_{i1})_{1 \leq i \leq r}, (t_{i2})_{1 \leq i \leq r}, (t_P)_{P \in \mathbb{P}}, (h_P)_{P \in \mathbb{P}} \right) \in K$$

satisfying the following conditions:

- (1) For each  $1 \leq i \leq r$ , we have  $t_{i1} \geq 0$  (resp.  $t_{i2} \geq 0$ ) whenever  $n_{i1} = 0$  (resp.  $n_{i2} = 0$ ).
- (2) For each  $P \in \mathbb{P}$ , the following congruences hold:

$$\begin{cases} n_{12}^P + n_{22}^P + n_{32}^P \equiv n_{11}^P + n_{21}^P + n_{31}^P \pmod{3}, \\ h_P + n_{11}^P + n_{21}^P + n_{31}^P \equiv 0 \pmod{2}, \\ h_P \equiv n_{11}^P + 2n_{21}^P - n_{12}^P + n_{22}^P \pmod{3}, \\ 3t_P \equiv n_{12}^P + n_{22}^P + n_{32}^P - n_{11}^P - n_{21}^P - n_{31}^P \pmod{6}. \end{cases}$$

By Remark 6.4, the set  $\Theta$  is well defined.

The following theorem is our first main result. It shows that the coordinates defined in Definition 7.1 parametrize the non-elliptic web diagrams in  $\Sigma_g$  for  $g \geq 2$ , and that the set of coordinates of all non-elliptic web diagrams in  $\Sigma_g$  is precisely the monoid  $\Theta$ .

We next introduce a definition that will be used in the proof of this theorem. A crossingless web diagram in  $\Sigma_g$  is called *almost non-elliptic* if it contains no 2-gons and no trivial loops as in (10).

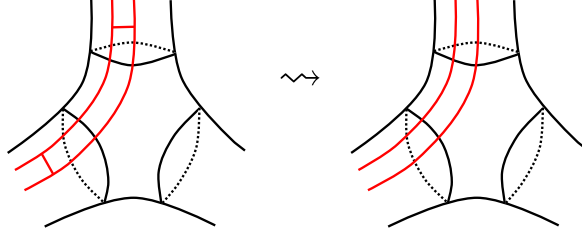


FIGURE 24. The procedure to remove 4-gons in  $W'$ .

**Theorem 7.4.** Let  $\mathcal{P} = \{C_j\}_{1 \leq j \leq r}$  be an oriented pants decomposition of  $\Sigma_g$  ( $g \geq 2$ ) with a dual graph  $\Gamma$ , where  $r = 3g - 3$ . The coordinate map

$$\kappa: B_{\Sigma_g} \longrightarrow \mathbb{N}^r \times \mathbb{N}^r \times \mathbb{Z}^r \times \mathbb{Z}^r \times \mathbb{Z}^{\mathbb{P}} \times \mathbb{Z}^{\mathbb{P}}$$

is injective, where  $B_{\Sigma_g}$  is defined in Definition 2.5 and  $\kappa$  is defined in Definition 7.1. Moreover,

$$\text{Im } \kappa = \Theta.$$

*Proof.* We first show that  $\text{Im } \kappa = \Theta$ . By Proposition 6.2, Theorems 5.10 and 6.3, we have

$$\text{Im } \kappa \subset \Theta.$$

Now let

$$\left( (n_{i1})_{1 \leq i \leq r}, (n_{i2})_{1 \leq i \leq r}, (t_{i1})_{1 \leq i \leq r}, (t_{i2})_{1 \leq i \leq r}, (t_P)_{P \in \mathbb{P}}, (h_P)_{P \in \mathbb{P}} \right) \in \Theta.$$

For each  $P \in \mathbb{P}$ , let

$$P' = P \setminus (\partial P \cap \Gamma).$$

By Proposition 6.2, Theorem 6.3, and Definition 7.3, there exists an essential non-elliptic web diagram  $W_P$  in  $P'$  such that

$$\mathbf{P}(W_P) = (n_{11}^P, n_{12}^P, n_{21}^P, n_{22}^P, n_{31}^P, n_{32}^P, t_P, h_P) \in \mathbb{Z}^{I(\Sigma_{0,3})},$$

where  $n_{jt}^P$  is defined in (35), the labeling of  $I(\Sigma_{0,3})$  is shown in Figure 4, and  $\mathbf{P}$  is defined in Definition 6.1.

For each  $1 \leq i \leq r$ , suppose that the annulus  $N(C_i)$  is adjacent to the pairs of pants  $P_1$  and  $P_2$  (possibly  $P_1 = P_2$ ). We identify

$$\mathcal{N}_i := N(C_i) \setminus (\partial N(C_i) \cap \Gamma)$$

with  $\mathbb{A}'$  (here  $\mathbb{A}'$  is obtained from the annulus by removing one point from each its boundary component), so that  $C_i$  is identified with the curve  $C$  in Figure 20, with orientations preserved. Then the quadruple  $(n_{i1}, n_{i2}, t_{i1}, t_{i2})$  uniquely determines a non-elliptic braided web  $W_i$  in  $\mathcal{N}_i$ , up to signature, by Theorem 5.10. There is a unique choice of signature for  $W_i$  that allows  $W_i$  to be glued compatibly with  $W_{P_1}$  and  $W_{P_2}$  when  $\mathcal{N}_i$  is glued to  $P_1$  and  $P_2$ .

After gluing all annuli  $N(C_i)$ ,  $1 \leq i \leq r$ , with all pairs of pants  $P \in \mathbb{P}$  to recover  $\Sigma_g$ , and simultaneously gluing all webs  $W_i$ ,  $1 \leq i \leq r$ , with the webs  $W_P$ ,  $P \in \mathbb{P}$ , we obtain an almost non-elliptic web diagram  $W'$  on  $\Sigma_g$ . This web may contain 4-gons, as illustrated in the left picture in Figure 24. By removing these 4-gons as in Figure 24, we obtain a non-elliptic web diagram  $W$ . By construction, it is immediate that

$$\kappa(W) = \left( (n_{i1})_{1 \leq i \leq r}, (n_{i2})_{1 \leq i \leq r}, (t_{i1})_{1 \leq i \leq r}, (t_{i2})_{1 \leq i \leq r}, (t_P)_{P \in \mathbb{P}}, (h_P)_{P \in \mathbb{P}} \right).$$

We now prove that  $\kappa$  is injective. Suppose that  $\kappa(W_1) = \kappa(W_0)$  for two non-elliptic web diagrams  $W_1$  and  $W_0$  in  $\Sigma_g$  that are in general position with respect to  $\mathcal{P}$ . Recall the graded algebra  $\mathcal{S}_{\mathcal{P}}(\Sigma_g)$  defined in (12). To show that  $W_1 = W_0$ , it suffices to prove that (Lemma 2.8)

$$[W_1] = [W_0] \in \mathcal{S}_{\mathcal{P}}(\Sigma_g).$$

For each  $P \in \mathbb{P}$ , Theorem 6.3(a) implies that  $W_1 \cap P$  can be obtained from  $W_0 \cap P$  by a sequence of moves shown in Figure 22, together with the moves obtained by rotating the pictures in Figure 22 by  $120^\circ$  and  $240^\circ$ . By repeatedly applying moves in Figure 25 to  $W_1$ , we obtain an almost non-elliptic web diagram  $W_2$  on  $\Sigma_g$  such that  $W_2 \cap P = W_0 \cap P$  for each  $P \in \mathbb{P}$ . Relations (5) and (6) then imply that

$$[W_1] = [W_2] \in \mathcal{S}_{\mathcal{P}}(\Sigma_g).$$

Let  $W_3$  be the web diagram obtained from  $W_2$  by removing all 4-gons in the annuli using the moves shown in Figure 16. Similarly, we have

$$[W_1] = [W_2] = [W_3] \in \mathcal{S}_{\mathcal{P}}(\Sigma_g).$$

Since all 4-gons in the annuli have been removed, Lemma 5.2(a) implies that  $W_3 \cap \mathcal{N}_i$  is a non-elliptic braided web. Because  $W_3 \cap P = W_0 \cap P$  for each  $P \in \mathbb{P}$ , the webs  $W_3 \cap \mathcal{N}_i$  and  $W_0 \cap \mathcal{N}_i$  have the same signature. Moreover,

$$\mathbf{t}(W_3 \cap \mathcal{N}_i) = \mathbf{t}(W_1 \cap \mathcal{N}_i) = \mathbf{t}(W_0 \cap \mathcal{N}_i),$$

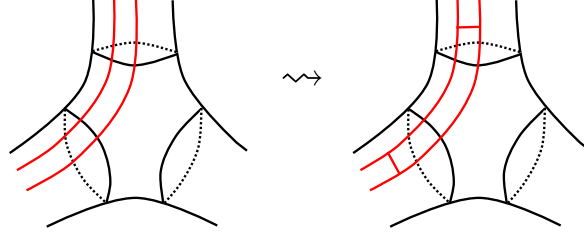
where  $\mathbf{t}$  is defined in Definition 5.8. By Theorem 5.10, it follows that

$$W_3 \cap \mathcal{N}_i = W_0 \cap \mathcal{N}_i \quad \text{for all } 1 \leq i \leq r.$$

Hence  $W_3 = W_0$ , and therefore

$$[W_1] = [W_2] = [W_3] = [W_0] \in \mathcal{S}_{\mathcal{P}}(\Sigma_g).$$

This completes the proof. □

FIGURE 25. The procedure to obtain  $W_2$ .

**7.2. The closed torus.** Let  $\gamma$  be an oriented closed curve in  $\Sigma_1$ , and fix a point  $p \in \gamma$ . A non-elliptic web diagram  $W$  on  $\Sigma_1$  is said to be in **general position** with respect to  $\gamma$  if  $W$  is in minimal intersection position with  $\gamma$  and  $p \notin W$ .

Cutting  $\Sigma_1$  along  $\gamma$  and taking the closure yields an annulus, which we denote by  $\mathbb{A}_\gamma$ . The point  $p$  gives rise to two points  $p', p'' \in \partial\mathbb{A}_\gamma$ , one on each boundary component. We write

$$\mathbb{A}'_\gamma := \mathbb{A}_\gamma \setminus \{p', p''\}.$$

Let  $W_\gamma$  denote the web diagram on  $\mathbb{A}'_\gamma$  obtained from  $W$  by cutting along  $\gamma$ . By Proposition 5.5(a), the web  $W_\gamma$  is a non-elliptic braided web on  $\mathbb{A}'_\gamma$ .

The orientation of  $\gamma$  induces orientations on the two boundary components of  $\mathbb{A}'_\gamma$ . There is a unique identification of  $\mathbb{A}'_\gamma$  with  $\mathbb{A}'$  such that the induced orientations of the boundary components of  $\mathbb{A}'_\gamma$  agree with the orientation of the curve  $C$  in Figure 20.

We now introduce the following coordinate for  $W$ .

**Definition 7.5.** *Define*

$$\kappa: B_{\Sigma_1} \longrightarrow \mathbb{N}^2 \times \mathbb{Z}^2, \quad W \longmapsto (n_1(W), n_2(W), t_1(W), t_2(W)) := \mathbf{t}(W_\gamma),$$

where  $\mathbf{t}$  is defined in Definition 5.8.

The following shows the well-definedness of  $\kappa$  in Definition 7.5.

**Lemma 7.6.** *The map  $\kappa$  defined in Definition 7.5 is well defined; that is, it is independent of the choice of the general position of  $W$  with respect to  $\gamma$ .*

*Proof.* It suffices to prove the following statement. Let  $\beta$  be another oriented closed curve in  $\Sigma_1$  parallel to  $\gamma$ , and fix a point  $c \in \beta$ . Then

$$\mathbf{t}(W_\gamma) = \mathbf{t}(W_\beta),$$

where  $W \in B_{\Sigma_1}$  is in general position with respect to both  $\gamma$  and  $\beta$ .

By Proposition 5.5(b), we have

$$n_1(W_\gamma) = n_1(W_\beta), \quad n_2(W_\gamma) = n_2(W_\beta).$$

The curves  $\gamma$  and  $\beta$  bound two annuli in  $\Sigma_1$ , which we denote by  $\mathbb{A}_1$  and  $\mathbb{A}_2$ . Set

$$\mathbb{A}'_1 := \mathbb{A}_1 \setminus \{p, c\}, \quad \mathbb{A}'_2 := \mathbb{A}_2 \setminus \{p, c\}.$$

By Proposition 5.5(a), the web  $W \cap \mathbb{A}'_1$  (resp.  $W \cap \mathbb{A}'_2$ ) is a non-elliptic braided web on  $\mathbb{A}'_1$  (resp.  $\mathbb{A}'_2$ ).

It follows immediately that

$$t_j(W_\gamma) = t_j(W \cap \mathbb{A}'_1) + t_j(W \cap \mathbb{A}'_2) = t_j(W_\beta), \quad j = 1, 2.$$

This proves the lemma.  $\square$

The following theorem is our second main result. It shows that the coordinates of non-elliptic web diagrams in the closed torus  $\Sigma_1$  parametrize these web diagrams.

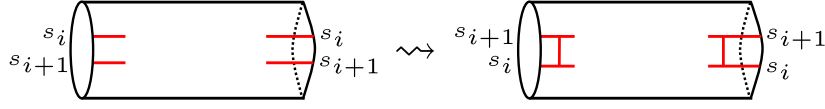


FIGURE 26. A move to swap signatures, where  $s_i \neq s_{i+1}$ .

**Theorem 7.7.** *Let  $\gamma$  be an oriented closed curve in  $\Sigma_1$ , and fix a point  $p \in \gamma$ . Then the map*

$$\kappa: B_{\Sigma_1} \longrightarrow \mathbb{N}^2 \times \mathbb{Z}^2$$

*is injective. Moreover,*

$$\text{Im } \kappa = \{(n_1, n_2, t_1, t_2) \in \mathbb{N}^2 \times \mathbb{Z}^2 \mid t_i \geq 0 \text{ if } n_i = 0, i = 1, 2\}. \quad (36)$$

*Proof.* We first prove the injectivity of  $\kappa$ . Suppose that  $\kappa(W) = \kappa(D)$  for any two  $W, D \in B_{\Sigma_1}$ . Then  $\mathbf{t}(W_\gamma) = \mathbf{t}(D_\gamma)$ .

Let

$$\mathbf{s}(W_\gamma) = (s_1, \dots, s_n, s_{n+1}, \dots, s_{2n}) \in \{-, +\}^{2n},$$

where  $\mathbf{s}$  is the signature defined in (30) and  $n = i(\gamma, W)$ . Since  $W_\gamma$  is obtained from  $W$  by cutting along  $\gamma$ , we have  $s_i = s_{n+i}$  for  $1 \leq i \leq n$ . By applying a sequence of moves in Figure 26, we obtain a braided web  $W_1$  on  $\mathbb{A}'_\gamma$  such that  $\mathbf{s}(W_1) = \mathbf{s}(D_\gamma)$ .

Let  $W_2$  be obtained from  $W_1$  by removing all 4-gons as in Figure 16. Then

$$\mathbf{t}(W_2) = \mathbf{t}(W_\gamma) = \mathbf{t}(D_\gamma), \quad \mathbf{s}(W_2) = \mathbf{s}(D_\gamma).$$

Lemma 5.2(a) and Theorem 5.10 therefore imply that  $W_2 = D_\gamma$ .

When gluing  $\mathbb{A}_\gamma$  along  $\gamma$  to recover  $\Sigma_1$ , we simultaneously glue  $W_1$  (resp.  $W_2$ ) to an almost non-elliptic web diagram  $W'_1$  (resp.  $W'_2$ ) in  $\Sigma_1$ . Since  $W_2 = D_\gamma$ , we have  $W'_2 = D$ . Relations (5) and (6) imply that

$$[W] = [W'_1] = [W'_2] = [D] \in \mathcal{S}_C(\Sigma_1),$$

where  $\mathcal{S}_C(\Sigma_1)$  is the graded algebra defined in (12). By Lemma 2.8, it follows that  $W = D$ .

We now prove (36). Theorem 5.10 shows that

$$\text{Im } \kappa \subset \{(n_1, n_2, t_1, t_2) \in \mathbb{N}^2 \times \mathbb{Z}^2 \mid t_i \geq 0 \text{ if } n_i = 0, i = 1, 2\}.$$

Conversely, let  $(n_1, n_2, t_1, t_2) \in \mathbb{N}^2 \times \mathbb{Z}^2$  satisfy  $t_i \geq 0$  whenever  $n_i = 0$  for  $i = 1, 2$ . Choose a signature  $\mathbf{a} = (a_1, \dots, a_n, a_{n+1}, \dots, a_{2n}) \in \{-, +\}^{2n}$  with  $a_i = a_{n+i}$  for  $1 \leq i \leq n$ . Theorem 5.10 guarantees the existence of a non-elliptic braided web  $E$  on  $\mathbb{A}'_\gamma$  such that

$$\mathbf{t}(E) = (n_1, n_2, t_1, t_2) \quad \text{and} \quad \mathbf{s}(E) = \mathbf{a}.$$

Gluing  $\mathbb{A}_\gamma$  along  $\gamma$  yields an almost non-elliptic web diagram  $E'$  in  $\Sigma_1$ . Let  $E''$  be the non-elliptic web diagram obtained from  $E'$  by removing all 4-gons; this procedure is unique and satisfies  $[E''] = [E']$ . Then

$$\kappa(E'') = \mathbf{t}(E''_\gamma) = \mathbf{t}(E) = (n_1, n_2, t_1, t_2),$$

completing the proof.  $\square$

## REFERENCES

- [CJK21] Suhyoung Choi, Hongtaek Jung, and Hong Chan Kim. Symplectic coordinates on  $PSL_3(\mathbb{R})$ -Hitchin components. *Pure and applied mathematics quarterly*, 16(5):1321–1386, 2021.
- [DS24] Daniel C Douglas and Zhe Sun. Tropical Fock–Goncharov coordinates for-webs on surfaces I: construction. In *Forum of Mathematics, Sigma*, volume 12, page e5. Cambridge University Press, 2024.
- [DS25] Daniel C. Douglas and Zhe Sun. Tropical Fock–Goncharov coordinates for  $SL_3$ -webs on surfaces II: naturality. *Algebraic Combinatorics*, 8(1):101–156, 2025.
- [FG06] Vladimir V. Fock and Alexander B. Goncharov. Moduli spaces of local systems and higher teichmüller theory. *Publ. Math. Inst. Hautes Études Sci.*, 103:1–211, 2006.

- [FG07] Vladimir V Fock and Alexander B Goncharov. Moduli spaces of convex projective structures on surfaces. *Advances in Mathematics*, 208(1):249–273, 2007.
- [FS22] Charles Frohman and Adam S Sikora.  $SU(3)$ -skein algebras and webs on surfaces. *Mathematische Zeitschrift*, 300(1):33–56, 2022.
- [Gol90] William M Goldman. Convex real projective structures on compact surfaces. *Journal of Differential Geometry*, 31(3):791–845, 1990.
- [Hig25] Vijay Higgins. Miraculous Cancellations and the Quantum Frobenius for  $SL_3$  Skein Modules. *International Mathematics Research Notices*, 2025(15):rnaf226, 2025.
- [IK24] Tsukasa Ishibashi and Shunsuke Kano. Unbounded  $\mathfrak{sl}_3$ -laminations around punctures. *arXiv preprint arXiv:2404.18236*, 2024.
- [IK25] Tsukasa Ishibashi and Shunsuke Kano. Unbounded  $\mathfrak{sl}_3$ -laminations and their shear coordinates. *Algebraic & Geometric Topology*, 25(3):1433–1500, 2025.
- [Kim99] Hong Chan Kim. The symplectic global coordinates on the moduli space of real projective structures. *Journal of Differential Geometry*, 53:359–401, 1999.
- [Kim20] Hyun Kyu Kim.  $SL_3$ -laminations as bases for  $PGL_3$  cluster varieties for surfaces. *arXiv preprint arXiv:2011.14765*, 2020.
- [KLW25] Hyun Kyu Kim, Thang TQ Lê, and Zhihao Wang. Frobenius homomorphisms for stated  $SL_n$ -skein modules. *arXiv preprint arXiv:2504.08657*, 2025.
- [Kup96] Greg Kuperberg. Spiders for rank 2 Lie algebras. *Communications in mathematical physics*, 180(1):109–151, 1996.
- [KW24] Hyun Kyu Kim and Zhihao Wang. The Unicity Theorem and the center of the  $SL_3$ -skein algebra. *arXiv preprint arXiv:2407.16812*, 2024.
- [LS04] Feng Luo and Richard Stong. Dehn-Thurston coordinates for curves on surfaces. *Communications in Analysis and Geometry*, 12(1-2):1–41, 2004.
- [MOY98] Hitoshi Murakami, Tomotada Ohtsuki, and Shuji Yamada. Homfly polynomial via an invariant of colored plane graphs. *Enseign Math*, 44(3):325–360, 1998.
- [PS00] Józef Henryk Przytycki and Adam S Sikora. On skein algebras and  $SL_2(\mathbb{C})$ -character varieties. *Topology*, 39(1), 2000.
- [Sik01] Adam Sikora.  $SL_n$ -character varieties as spaces of graphs. *Transactions of the American Mathematical Society*, 353(7):2773–2804, 2001.
- [SW07] Adam Sikora and Bruce Westbury. Confluence theory for graphs. *Algebraic & Geometric Topology*, 7(1):439–478, 2007.
- [SWZ20] Zhe Sun, Anna Wienhard, and Tengren Zhang. Flows on the  $PGL(V)$ -Hitchin component. *Geometric and Functional Analysis*, 30(2):588–692, 2020.
- [Tur88] VG Turaev. The Conway and Kauffman modules of a solid torus, *Zap. Nauchn. Sem. Leningrad. Otdel. Mat. Inst. Steklov.(LOMI)*, 167:79–89, 1988.
- [Tur89] V.G. Turaev. *Algebra of loops on surfaces, algebra of knots, and quantization*, volume 9 of *Adv. Ser. Math. Phys.*, pages 59–95. World Sci. Publ., Teaneck, NJ, 1989.

ZHE SUN, SCHOOL OF MATHEMATICAL SCIENCES, UNIVERSITY OF SCIENCE AND TECHNOLOGY OF CHINA, 96 JINZHAI ROAD, 230026 HEFEI, CHINA

*Email address:* sunz@ustc.edu.cn

ZHIIHAO WANG, SCHOOL OF MATHEMATICS, KOREA INSTITUTE FOR ADVANCED STUDY (KIAS), 85 HOEGI-RO, DONGDAEMUN-GU, SEOUL 02455, REPUBLIC OF KOREA

*Email address:* zhihaowang@kias.re.kr